frontiers in Marine Science

TYPE Original Research
PUBLISHED 30 July 2026
DOI 10.3389/fmars.2026.1901130

OPEN ACCESS

EDITED BY
Ioannis A. Giantsis,
Aristotle University of Thessaloniki, Greece

REVIEWED BY
Banghua Xia,
Shandong University, Weihai, China
Yanghua Qu,
Nutrition and Health Research Institute, COFCO, China

*CORRESPONDENCE
Raffaella Boggia
raffaella.boggia@unige.it

†These authors have contributed equally to this work

RECEIVED 05 June 2026
REVISED 30 June 2026
ACCEPTED 02 July 2026
PUBLISHED 30 July 2026

CITATION
Randazzo B, Miccoli A, Caccamo L, Gai F, Boggia R, Turrini F, Leone A, Carboni S, Concu D and Maricchiolo G (2026) Dietary black soldier fly meal remodels hepatic lipid metabolism and fillet fatty acids profile of flathead grey mullet *Mugil cephalus* (Linnaeus, 1758). *Front. Mar. Sci.* 13:1901130. doi: 10.3389/fmars.2026.1901130

Dietary black soldier fly meal remodels hepatic lipid metabolism and fillet fatty acids profile of flathead grey mullet *Mugil cephalus* (Linnaeus, 1758)

Basilio Randazzo[1,2†], Andrea Miccoli[3†], Letteria Caccamo[1,2], Francesco Gai[2,4], Raffaella Boggia[2,5*], Federica Turrini[2,5], Antonella Leone[2,6], Stefano Carboni[7], Danilo Concu[7] and Giulia Maricchiolo[1,2]

[1]Institute for Marine Biological Resources and Biotechnology, National Research Council, Messina, Italy, [2]National Biodiversity Future Center (NBFC), Palermo, Italy, [3]Institute for Marine Biological Resources and Biotechnology, National Research Council, Ancona, Italy, [4]Institute of Sciences of Food Production, National Research Council, Grugliasco, Italy, [5]Department of Pharmacy, University of Genova, Genova, Italy, [6]Institute of Sciences of Food Production, National Research Council, Lecce, Italy, [7]International Marine Centre (IMC), Oristano, Italy

The effect of dietary black soldier fly (*Hermetia illucens*) meal on flathead grey mullet (*Mugil cephalus*) liver transcriptomic response and fillet quality was assessed. To this end, 360 juvenile flathead grey mullets (weight = 40.2 ± 0.5 g) were randomly divided into four experimental groups. Fish were fed a reference diet (BSF0) and three experimental diets in which graded levels of partially defatted black soldier fly meal were used as protein source (BSF10, BSF15, and BSF20). A dose-dependent transcriptional response to insect meal inclusion was evident on the modulation of differentially expressed genes (DEGs). While BSF10 did not result in significant transcriptomic changes, functional analyses of the hepatic transcriptome highlighted strong impacts at metabolic, endocrine, and immune levels at 20% BSF inclusion. A metabolic switch from glycolytic flux toward oxidative fatty acid catabolism, as a consequence of dietary BSF meal, was found, altogether indicating a remodeling of the hepatic circadian–metabolic axis. Moreover, the consistent upregulation of the pathways involved in the control of protein folding and oxidative phosphorylation suggested an attempt to maintain cellular homeostasis, particularly in the BSF20 group. Chemical analyses revealed a comparable protein and lipid content of the final edible product across the groups, indicating that up to 20% dietary protein replacement with BSF is nutritionally sustainable. However, lauric acid (12:0) represented the most indicative FA in fillet of fish fed BSF-based diets, and an inverse proportion of palmitic acid (16:0) content between the diet and fillet composition was observed in fish fed experimental diets. The increase in n3 FAs, including docosahexaenoic acid (22:6n3, DHA) in fillets from the BSF20 group, indicates metabolic adaptations in response to a dietary decrease of such FAs. Together, the results obtained herein indicate that *M. cephalus* can accommodate partial replacement of dietary

conventional protein sources with BSF meal, with no adverse effects on the quality of the final edible product. However, longer-term feeding trials are needed to assess a long-term use of BSF-based diets on cellular metabolic imbalances, as finely unveiled by the transcriptomic shift induced by 20% replacement.

KEYWORDS

fatty acids, *Hermetia illucens*, liver, muscle, transcriptome

1 Introduction

Global aquaculture has exceeded 130 million tons of annual production, cementing its position as the fastest-growing food sector worldwide (FAO, 2024). Yet, this remarkable expansion has long uniquely relied on fishmeal (FM), a finite marine-derived protein source whose costs are rising, supply is inconsistent, and ecological footprint is substantial (Olsen and Hasan, 2012).

While high-value carnivorous species such as Atlantic salmon (*Salmo salar*), European seabass (*Dicentrarchus labrax*), and gilthead seabream (*Sparus aurata*) have long dominated commercial aquaculture, their intrinsically high FM requirements have created a structural bottleneck that persists despite decades of research into plant-based protein replacements (Asche and Tveterås, 2004; Baruah et al., 2017; Macusi et al., 2023). The consequence is a sector that remains partially dependent on wild-capture fisheries, a paradox of intensification rather than true sustainability, and a particularly acute stagnation in the European aquaculture industry (Guillen et al., 2025). An underexplored approach to improve the resilience and sustainability of finfish production is to redirect commercial interest toward the production of species that require minimal FM in their diets.

In this perspective, the flathead grey mullet (*Mugil cephalus*) is a euryhaline, omnivorous, and low-trophic fish species, with a low dietary FM requirement and a high nutritional value for human consumption (Whitfield et al., 2012). Moreover, its tolerance to wide environmental variability is particularly relevant under accelerating global climate change, where farming conditions are increasingly unpredictable (Crosetti, 2015). The flathead grey mullet production has globally increased in recent years, with 5,934 tons deriving by aquaculture in 2024 (Vallainc et al., 2026). Traditionally, flathead grey mullet is farmed in extensive systems relying on natural diet supplemented with feeds formulated for other species (Oren, 1981; Biswas et al., 2012; Essa, 1996; Mondall et al., 2015), and its specific nutritional requirements remain poorly characterized (Bertini et al., 2023).

Over the last decade, research advances in fish nutrition have explored a large set of alternative protein sources aiming at replacing conventional ingredients in aquafeed formulations. Among these, insect meal has gained great interest owing to its high protein content and essential amino acidic profile, similar to that of FM (Caligiani et al., 2018; Makkar et al., 2014; Smetana et al., 2019; Nairuti et al., 2021) and its low ecological footprint in terms of land use, water consumption, and CO_2 emission. In particular, the black soldier fly (*Hermetia illucens*, BSF) has been recognized as a good protein and mineral source, and is rich in bioactive compounds, including chitin, antimicrobial peptides, and medium-chain fatty acids (FAs), which have been shown to exert species-specific positive effects on fish health, gut integrity, and immune function (Gasco et al., 2018; Nogales-Mérida et al., 2019; Randazzo et al., 2023). However, the lipid composition of BSF meal is characterized by an unbalanced FA profile compared to FM, displaying a high proportion of saturated fatty acids (SFAs) compared to polyunsaturated fatty acids (PUFAs), particularly the nutritionally essential omega-3 content, which may limit its use in fish diets (Renna et al., 2017; Belghit et al., 2018, 2019; Mancini et al., 2018; Bruni et al., 2020). Even though BSF FA profile can be partially modeled by the growing substrate (Mendez Sanchez et al., 2025), it remains one of the main conditioning factors limiting its extensive use in aquafeed formulations. This imbalanced FA profile carries potential negative consequences for fish physiology and may compromise the nutritional quality of the edible fillet, a critical concern for both fish welfare and consumer acceptability (Seierstad et al., 2009; Caballero-Solares et al., 2017; Eslamloo et al., 2017), particularly when it comes to underexplored fish species. Moreover, the species-specific capacity of fish to use or *de novo* bioconvert short-chain precursors into PUFAs such as eicosapentaenoic acid (EPA) and docosahexaenoic acid (DHA) varies considerably and is generally limited in euryhaline and marine species (Tocher, 2003; Turchini et al., 2009; Marrero et al., 2024), making the prediction of diet-induced FA remodeling in *M. cephalus* particularly uncertain.

The liver is the central area through which lipid signals are transduced into physiological outcomes. This is the primary tissue for FA uptake, elongation, desaturation, and *de novo* lipogenesis, and simultaneously acts as a front-line organ in detoxification, innate immunity, and protein synthesis and degradation (Houlihan et al., 1986; Carter et al., 2001; Tocher, 2003; Bakke et al., 2010; Du et al., 2014; Heymann and Tacke, 2016; Wu et al., 2016). Crucially, a substantial number of hepatic genes are directly regulated by dietary intake, making the liver transcriptome a relevant information source on the animal physiological status. In recent years, the establishment of next-generation RNA sequencing (RNA-seq) and the curation of bioinformatic resources and annotation portals have revolutionized the capacity to investigate and interpret functional genomics also in non-model species (Salem et al., 2010; Calduch-Giner et al., 2013; Magnanou et al., 2014; Fox et al., 2014; Mu et al., 2010, 2014). The recent release of a chromosome-level genome assembly for *M. cephalus* now allows for such genome-wide investigations in this species, removing a key technical barrier that had previously limited mechanistic nutritional research in

grey mullet. To date, only one study explored the suitability of BSF meal in diets specifically formulated for *M. cephalus*, identifying a threshold beyond which fish growth and health were negatively affected (Randazzo et al., 2026). However, the concurrent effects of increasing BSF meal inclusion on both the hepatic transcriptional response and the nutritional quality of the final product for human consumption remain entirely uncharacterized in this species. In the present study, juvenile flathead grey mullets were fed four isoproteic, isolipidic, and isoenergetic diets, i.e., a low-FM reference formulation and three diets in which BSF prepupae meal progressively replaced conventional protein sources at 10%, 15%, and 20% substitution levels, for 138 days. In a previous study performed on the same experiment and fish batch, no adverse effect on fish growth was reported and only marginal impairment of gut health was histologically observed at the highest BSF inclusion (Randazzo et al., 2026). Herein, on fish from the same cohort used in the previous study, liver transcriptome was analyzed by RNA-seq, and fillet FA profiles were characterized by gas chromatography–mass spectrometry (GC/MS). By integrating liver gene expression and transcriptome functional analyses with fillet lipid composition, this work provides the first multi-dimensional assessment of the physiological and product-quality consequences of BSF meal inclusion in *M. cephalus* diet, contributing to the evidence base needed to design nutritionally optimized and ecologically sustainable diets for this emerging aquaculture species.

2 Materials and methods

2.1 Ethics

The feeding trial experiment and all the procedures involving animals were carried out in strict accordance with EU legal frameworks relating to the protection of animals used for scientific purposes (Directive 2010/63/EU). It was approved by the Italian Ministry of Health (n. 5598B.N.T61).

2.2 Experimental diets

Four practical pelleted diets were formulated to be grossly isoproteic, isolipidic, and isoenergetic, as reported in Table 1. A diet (BSF0), based on conventional animal and plant protein sources, i.e., FM, poultry meal (PM), feather meal (FtM), and soybean meal (SBM), was used as reference, according to diets formulated by Bertini and colleagues (2023). Three other diets were formulated by replacing 10%, 15%, and 20% (BSF10, BSF15 and BSF20) of the ingredients conventionally used as protein sources (FM, PM, FtM, and SBM) in the reference diet with partially defatted BSF prepupae meal; FM, PM, FtM, and SBM were equally replaced at increasing BSF meal inclusion. Details on diets preparation are reported in previous research (Randazzo et al., 2026).

TABLE 1 Ingredients (g 100 g^{-1}) of the experimental diets used for the feeding trial. .

	BSF0	BSF10	BSF15	BSF20
Ingredients (g 100 g^{-1})				
BSF (*Hermetia illucens*) meal[1]	0.0	4.8	7.2	9.6
Fish meal[2]	3.0	1.8	1.2	0.6
Poultry meal[3]	10	8.8	8.2	7.6
Feather meal (hydrolysate)[4]	5.0	3.8	3.2	2.6
Soybean meal[5]	30	28.8	28.2	27.6
Wheat meal	40	40	40	40
Soybean oil	3.0	3.0	3.0	3.0
Cod liver oil	3.5	3.5	3.5	3.5
L-lysine	0.85	0.85	0.85	0.85
DL-methionine	0.3	0.3	0.3	0.3
L-tryptophan	0.1	0.1	0.1	0.1
Vitamin e50[6]	0.05	0.05	0.05	0.05
Vitamin-mineral premix[7]	1.0	1.0	1.0	1.0
Dicalcium phosphate	3.0	3.0	3.0	3.0
Antioxidant mix[8]	0.2	0.2	0.2	0.2

[1]Partially defatted *Hermetia illucens* meal (DM 92.01%, CP, 47.3%; CF, 14.1%, crude fiber 12.40%, ash 10.24% as fed).
[2]Fish meal (CP, 59,5%; CF, 11% as fed), KÖSTER MARINE PROTEINS GMBH.
[3]Poultry meal (CP, 65%; CF, 14.5% as fed), ECB, Saria®.
[4]Feather meal (CP, 80.5%; CF, 10% as fed), ECB, Saria®.
[5]High protein soybean meal, non-GMO (CP, 46.5%; CF, 1.5% as fed), BUNGE©.
[6]ROVIMIXE50, DSM Nutritional Products, Grenzach, Germany.
[7]Vitamins and mineral premix (mg kg^{-1} diet, Naturalleva, Cologna Veneta, Italy): D 0.05 mg, A 2.37 mg, E 323.9 mg, inositol 158.0 mg, niacin 182.7 mg, pantothenic acid 67.6 mg, B2 27.4 mg, B1 27.7 mg, B6 24.27 mg, folic acid 6.52 mg, K 5.37 mg, biotin 0.96 mg, B12 0.05 mg, choline 1,314.58 mg, C 250.25 mg, calcium 0.72 mg, cobalt 0.30 mg, copper 48.62 mg, iron 494.7 mg, magnesium 21.2 mg, manganese 25.89 mg, molybdate 0.97 mg, nickel 0.80 mg, phosphorus 0.51 mg, potassium 0.83 mg, sodium 0.14 mg, selenium 0.83 mg, sulfur 0.35 mg, and zinc 52.7 mg.
[8]Propyl gallate (Naturalleva, Cologna Veneta, Italy): 9.9%; B.H.A.: 5.0%, ethoxyquin: 9.9%; citric acid: 11.0%; Carrier(=SiO^2) ad100%.

2.3 Fish rearing, feeding trial, and sampling

Three hundred and eighty juvenile flathead grey mullet (*M. cephalus)* (weight = 40.2 ± 0.5 g), produced at the International Marine Centre (IMC, Oristano, Italy) according to the protocols described by FAO Fisheries and Aquaculture Technical Paper, No. 699 (Vallainc et al., 2026), were transferred to the experimental aquaculture facility of the Institute for Marine Biological Resources and Biotechnology of the National Research Council (IRBIM-CNR, Messina, Italy). After 1 week of acclimation, 20 randomly chosen specimens were sacrificed with an overdose of anaesthetic (Tricaine Pharmaq 500 mg L^{-1}) to assess the initial health conditions in the original batch by visual inspection and histological analyses of target organs as described in section 2.5. The remaining fish (n = 360) were randomly divided into 12 experimental tanks (n = 30 each tank). The tanks were connected to a flow-through system in which incoming sea water were sand filtered and sterilized by means of an ultraviolet (UV) lamp; the system was set to guarantee 24 daily complete renewals and a natural photoperiod was adopted. Fish were assigned to the four dietary treatments, in triplicate and fed the experimental diets (BSF0, BSF10, BSF15, and BSF20) for 138 days. Feeding ratio was adjusted in all the treatments according to the water temperature (1%–3% body weight).

Fish from all the tanks were bulk-weighted monthly to adjust the amount of feed per tank. Fish were hand-fed in three daily meals (8:00, 12:00, and 16:00). Water parameters were measured daily (temperature, 20.3 ± 3.9 °C; O_2, 6.65 ± 0.8 mg L^{-1}; salinity, 39.07 ± 0.41 PSU; pH, 8.62 ± 0.42). Experimental tanks were daily cleaned by syphoning to remove feces and uneaten feed. At the end of the feeding trial, after euthanasia (Tricaine Pharmaq 500 mg L^{-1}), fish were individually weighed and dissected for liver and fillet sampling. To avoid any circadian-related conditionings, all sampling procedures were performed in the morning (8:30–12:00 a.m.).

For chemical analyses, nine fish from each dietary group (n = 3 per tank) were used. Two fillets for each specimen were obtained using an appropriate sharp knife and placed in plastic bags; samples were immediately stored at −80 °C until freeze-drying.

Nine other fish for each dietary group (n = 3 per tank) were used for the transcriptomic analyses. Small pieces of hepatic tissue were sampled, placed in sterile 1. 5-mL vials and stored at −80 °C, until RNA extraction.

2.4 RNA preparation and sequencing

Liver tissue was collected from three individual fish per tank (nine per treatment total). Equal amounts of tissue (~15 mg per individual) were pooled within each tank to produce one ~ 45-mg composite sample per tank, yielding three pooled biological replicates per dietary group. Pooling was thus performed within-tank to reduce individual stochasticity and improve representation of the group-level transcriptional signal, while preserving tank-level biological independence required for differential expression statistics. Pooled samples were extracted using the RNeasy Mini Kit (Qiagen, Hilden, Germany), following the manufacturer's recommendations. RNA purity and concentration were assessed spectrophotometrically (NanoDrop® ND-1000, Wilmington, USA), while RNA quality was visualized on a 1% (w v^{-1}) agarose gel by staining of 28S and 18S ribosomal RNA bands with EuroSafe Nucleic Acid Stain (Euroclone spa, Milan, Italy). RNA-seq libraries were produced using the Lexogene QuantSeq 3′mRNA protocol and sequenced using an Illumina NovaSeq X Plus platform with the 150SE strategy. Library preparation and sequencing was outsourced to Personal Genomics (Verona, Italy). The average sequencing depth achieved was 19,881,444 raw reads per library, with a minimum of 17,835,416 and a maximum of 21,816,670 reads across libraries.

2.5 RNA-seq data processing

Raw sequencing data, deposited in the EBI ArrayExpress portal (accession ID E-MTAB-16923), were quality-checked and trimmed to remove residual adapters, low-quality nucleotides with a base caller quality threshold set at 0.05, ambiguous nt, poly(A) and poly (G) sequences, and homopolymers from the 3′ end. Trimmed reads were then mapped to the *M. cephalus* reference genome (NCBI ID GCF_022458985.1) using Dragen (version 3.9.5). Transcription was quantified at the gene level with featureCounts v 2.0.8 exploiting BAM files and the species' gff annotation file, to which 3′ and 5′ UTR features had been previously inferred from the gene, mRNA, exon, and CDS features with the NCBI script "add_utrs_to_gff.py" (python script available at https://ftp.ncbi.nlm.nih.gov/genomes/TOOLS/add_utrs_to_gff/).

M. cephalus annotation resources [i.e., mapping between NCBI gene ID and (i) gene name/description, (ii) gene ontology terms, and (iii) Kyoto Encyclopedia of Genes and Genomes (KEGG) pathways] were generated from the NCBI gff file (GCF_022458985.1_CIBA_Mcephalus_1.1_genomic.gff), gaf (GCF_022458985.1_CIBA_Mcephalus_1.1_gene_ontology.gaf) and obo files (https://geneontology.org/docs/download-ontology/), and in bash and R environments with custom shell commands and R scripts using the ontologyIndex, KEGGREST, and EnrichmentBrowser packages (scripts for data manipulation and processing available upon request to AM).

Differential gene expression analysis was conducted in R using the R DESeq2 package v 1.50.2, setting the control diet (BSF0) as reference level in each of the three pairwise comparisons (i.e., BSF10/BSF15/BSF20 vs. BSF0). Raw estimated counts of gene expression were normalized to sequencing depth and RNA composition with the median of ratios method. To increase the statistical power of differentially expressed gene (DEG) detection, only genes with at least 12 reads across the four experimental groups were maintained in the dataset. An independent filtering based on the mean of normalized counts for each gene was applied with a false discovery rate (FDR) cutoff of 0.05. Genes displaying extreme outliers and below the low mean threshold were filtered out from the dataset.

Gene Set Enrichment Analysis (GSEA) was run on KEGG pathways using clusterProfiler v 4.18.4 (function "fgsea") (Korotkevich et al., 2021), ranking the entire gene dataset tested for significance with DESeq2 using the formula sign($\log_2$FC) * (−$\log_{10}$(p-value)) (Reimand et al., 2019), and sorting it in descending numerical order. Data manipulation, computation, and visualization were performed in the RStudio environment with the

following packages: aplot v.0.2.9 (Xu et al., 2025), clusterProfiler v.4.18.4 (Xu et al., 2024), DEGreport v.1.46.0 (Pantano, 2026), DESeq2 v.1.50.2 (Love et al., 2014), enrichplot v.1.30.4 (Yu, 2025), ggrepel v.0.9.6 (Slowikowski, 2024), ggridges v.0.5.7 (Wilke, 2025), KEGGREST v.1.50.0 (Tenenbaum and Maintainer, 2025), pathview v.1.50.0 (Luo and Brouwer, 2013), R.utils v.2.13.0 (Bengtsson, 2025), RColorBrewer v.1.1-3 (Neuwirth, 2022), stringr v.1.6.0 (Wickham, 2025), tidyverse v.2.0.0 (Wickham et al., 2019), tximport v.1.38.2 (Soneson et al., 2015), VennDiagram v.1.8.2 (Chen and Boutros, 2011).

2.6 Proximate composition and fatty acid profile of diets and fillets

For the experimental diets, moisture content was determined by oven drying at 103 °C to constant weight according to AOAC Official Method 950.46 (AOAC, 2019). Ash content was determined by incineration at 550 ± 10 °C to constant mass following ISTISAN 96/34 guidelines (1996). Crude protein content was determined by the Kjeldahl method ($N \times 6.25$) according to ISTISAN 96/34 (1996). Total lipids were determined by Soxhlet extraction using petroleum ether (40–60 °C). For fatty acid methyl ester (FAME) analysis, lipids were additionally extracted using a cold extraction procedure based on the method of Bligh and Dyer (1959).

For the fillets, before analyses, samples were freeze-dried using a COOLSAFE 55–4 freeze dryer (LaboGene ApS, DK-3450 Allerød) for 72–96 h. Once freeze-drying was completed, each individual sample was immediately vacuum-packed and then kept at −80 °C until analyses. Freeze-dried fillets were ground with a knife mill (Grindomix GM200; Retsch GmbH, Haan, Germany) to determine their proximate composition, according to the same procedures implemented for feed analyses. Total lipid fractions were subjected to transesterification for FA profiling by GC–MS following Leone et al. (2015), with minor methodological modifications.

Briefly, total lipid extracts were saponified with 3 ml mL of 0.5 M NaOH in methanol, at 100 °C for 5 min. Forty-nine microliters of 1.0 mg mL^{-1} of methyl-tricosanoate (Sigma-Aldrich, Milan, Italy) was added as internal standard. The FA s were methylated by adding 2 mL of 14% Boron trifluoride (BF_3) (Sigma-Aldrich, B1252) in methanol and treated at 100 °C for 30 min. After cooling, hexane (1 mL) was added and vigorously stirred for 30 s before the addition of 1 mL of sodium chloride solution (0.6%). The esterified samples were placed at 4 °C for a better phase separation. After collecting the supernatant, another 1.0 mL of hexane was added, and the resulting mixture was vortexed. Finally, the combined extracts were evaporated under a nitrogen stream, and then the dried samples were dissolved in 1.0 mL of hexane and 3 µL was injected for GC/MS.

The analyses were performed on a GC-MS system consisting of a Shimadzu GC-17A version 3.0 coupled with MS QP5050A. Compounds were separated on a DB-5 capillary column having 30 m length, 0.25 mm ID (internal diameter), and 0.25 µm thickness. The GC-MS separation parameters were as follows: starting temperature at 160 °C, increases at 3 °C/min up to 240 °C, and holds at 240°C for 30 min. Split injection was conducted with a split ratio of 5:1, mobile phase was high-purity (99.999%) helium gas at a constant flow rate of 1.0 mL/min. Injector temperature was 250 °C. The MS detection conditions were as follows: MS source set at 250 °C and MS quadruple set at 150 °C. Electron ionization in positive mode (EI +); electron energy, 70 eV; scanning method of acquisition ranging from 30 to 450, for mass/charge (m/z) was optimized. Compounds were identified by using online the National Institute of Standards and Technology (NIST 14) library spectra and verified using reviewed literature.

2.7 Statistics

RNA-seq $\log_2$ fold change estimates were tested for statistical significance using the Wald test implemented in DESeq2, with the null hypothesis of no differential expression across the experimental diets (i.e., LFC = 0) for each gene, and shrunk using the apeglm method, v. 1.22.0 for visualization purposes. A Likelihood Ratio Test was also run in DESeq2 using the reduced formula of the linear model ~1 with the null hypothesis of the full model ("~feed") fitting as well as the reduced one. Genes exhibiting similar expression patterns across experimental groups were clustered into groups with the DEGreport package v. 1.36. Minimum gene abundance for grouping purposes was set to 10 (*minc* argument, default to 15).

GSEA (function "fgsea" of the clusterProfiler library) was run with a significance FDR threshold of 0.05.

For the statistical analyses of the fillet proximate composition and FA profile, the tank was considered as the experimental unit. Upon verifying the normality and homogeneity of the data via the Shapiro–Wilk and Levene tests, data were subjected to one-way analysis of variance (ANOVA) using the Graph software package Prism5 (Graph Pad Software, La Jolla, CA, USA). Results are reported as mean ± SD of tank means (n = 3 tanks per dietary group). In all tests, a p-value equal to or less than 0.05 was considered statistically significant.

3 Results and discussion

3.1 Differential gene expression and gene set enrichment analyses

Differential expression analysis was performed by comparing hepatic transcript abundance in fish fed dietary BSF inclusion (BSF10, BSF15, and BSF20) against the control group (BSF0) and revealed a clear dose-dependent transcriptional response to insect meal inclusion (Figure 1A; Supplementary Table S1). The 10% BSF meal replacement did not cause any significant transcriptional change compared to the control group; 27 (7 up- and 20 downregulated, accounting for the 0.041% and 0.12% of all genes tested) and 258 genes (109 up- and 149 downregulated, accounting for the 0.64% and 0.88% of all tested genes) were instead found differentially expressed (DE) as a consequence of 15% and 20% replacement of conventional ingredient with BSF meal, respectively. In addition to DEG abundance, dose dependency was evident in terms of effect size modulation, with BSF15/BSF20 vs. BSF0 pairwise comparison $\log_2$FC ranging between −4.10 and 2.46 (median, −1.04), and −9.80 and 3.34 (median, 0.889), respectively (Figure 1B). These data suggest that a transcriptional "tipping point " occurs between 10% and 15% replacement, with dramatic amplification at 20%,

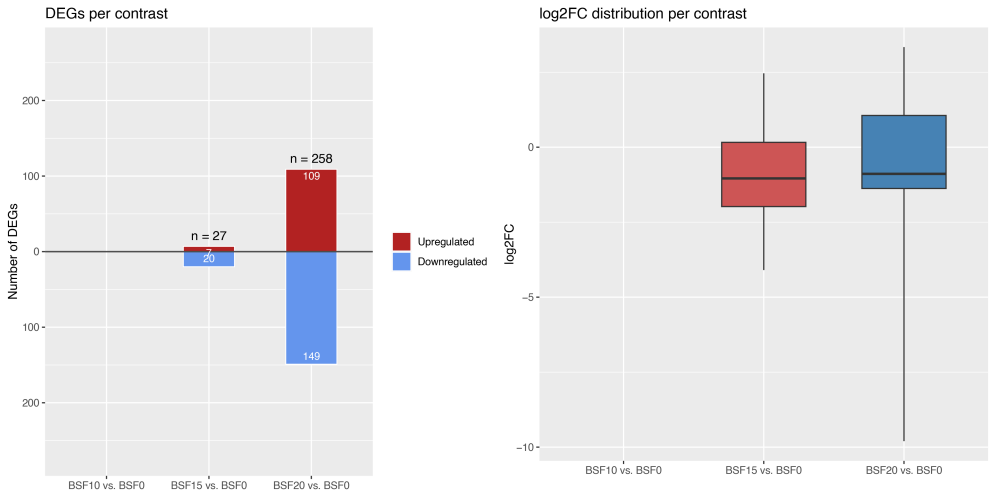

FIGURE 1
Number and $\log_2$ fold change distribution of differentially expressed genes (DEGs) across BSF dietary treatment contrasts. (left) Stacked bar chart showing the total number of DEGs in each pairwise comparison relative to the control (BSF0), separated by direction of regulation (red = upregulated, blue = downregulated). (right) Box plots displaying the $\log_2$ fold-change ($\log_2$FC) distribution of DEGs for the BSF15 vs. BSF0 and BSF20 vs. BSF0 contrasts.

and that hepatic metabolic reconfiguration begins at intermediate replacement levels and intensifies with higher insect meal inclusion. The absence of negative impairment on fish growth, as demonstrated in a previous study on the same experiment and fish batch (Randazzo et al., 2026), suggests either that compensatory homeostatic mechanisms are occurring in fish or that the feeding trial duration was not long enough to translate such transcriptional remodeling into a phenotypic outcome. Very few studies investigated the transcriptional responses of farmed animals to novel dietary ingredients, at either the systemic (i.e., whole-animal) or tissue level, and never in *M. cephalus*, so the present findings can only be cautiously compared to literature data. Nevertheless, the lack of any significant transcriptional variation in *M. cephalus* fed the BSF10 diet is consistent with observations in rainbow trout, where a dietary 10% BSF inclusion, either full-fat or defatted, elicited only a single hepatic DEG, with no effects on oxidative stress markers, heat shock proteins, or any of 21 plasma biochemical parameters investigated (Borland et al., 2024). These findings, despite being drawn across two phylogenetically distant teleost species investigated with an uneven degree of detail, suggest that the hepatic transcriptome can accommodate low-level BSF meal inclusion without mounting a substantial transcriptional response.

Sixteen genes were significantly modulated in BSF15 and BSF20 groups, both showing 100% concordant regulation direction (Figure 2A). Such conserved hepatic response to insect meal included the following: (i) *nr1d1* [NCBI gene ID 124997586, nuclear receptor subfamily 1, group d, member 1; $\log_2$FC −2.43 (BSF15) and −4.79 (BSF20)], which encodes for a ligand-sensitive transcription factor that represses the expression of core clock proteins, in turn relaying circadian signals into lipid metabolism, bile acid metabolism, and glucose metabolism; (ii) *nr0b2a* [NCBI gene ID 125017043, nuclear receptor subfamily 0, group B, member 2a; $\log_2$FC 0.97 (BSF15) and 0.98 (BSF20)], encoding for a negative regulator of receptor-dependent signaling pathways that is an essential component of the liver circadian clock regulating hepatic lipid metabolism in coordination with NR1D1 and RORG; (iii) *ciarta* [NCBI gene ID 125019847, circadian associated repressor of transcription a; $\log_2$FC −1.42 (BSF15) and −1.64 (BSF20)], whose product is a transcriptional repressor of the BMAL1–CLOCK complex negatively regulating the circadian transcription–translation feedback loop impacting on glucocorticoid sensitivity, metabolism, and immunity; and (iv) *pdk2a* [NCBI gene ID 125022539, pyruvate dehydrogenase kinase 2a; $\log_2$FC 1.51 (BSF15) and 2.34 (BSF20)], which encodes for a mitochondrial matrix enzyme enabling the kinase activity of the mitochondrial pyruvate dehydrogenase complex that oxidizes FA or glucose, overall indicating a metabolic shift toward lipid oxidation (Zhang et al., 2014; Jin et al., 2023).

Of these shared DEGs, *pdk2a* and *nr1d1* were among the top 20 most significantly differentially modulated genes based on *p*-adjusted, together with LOC124999164 (i.e., 18S ribosomal RNA) and *myca* (MYC proto-oncogene, bHLH transcription factor a), whose product is a master regulator of cellular metabolism by acting on ribosome biogenesis, lipid synthesis, nucleic acid synthesis, intermediary metabolism, and cell growth and proliferation (Le and Dang, 2014) (Figure 2B).

The 301 significant genes resulting from LRT, whose expression changed in any direction across the four experimental groups, were partitioned into six clusters based on their expression trajectory as per the logarithmic *Z*-score of gene abundance (Figure 3; Supplementary Table S2). Group 3 encompassed 104 genes exhibiting a smooth, dose-dependent repression that emerges above the 10% BSF replacement threshold. The most statistically significant genes in this cluster were *map9*, *myca*, *c7b*, *nr1d1*, *pnpla3*, *ldlra*, *slc1a3a*, and *dio2*. Biologically, this cluster includes some genes expressed in the nucleus that share the molecular function of enabling RNA polymerase II cis-regulatory region sequence-specific DNA binding (GO:0000978). Genes in this cluster are also involved in the suppression of hepatic metabolic, endocrine, and immune functions —including innate immunity (e.g., *c7b* and *socs3b* control the complement activation pathway, and neutrophil production

10.3389/fmars.2026.1901130

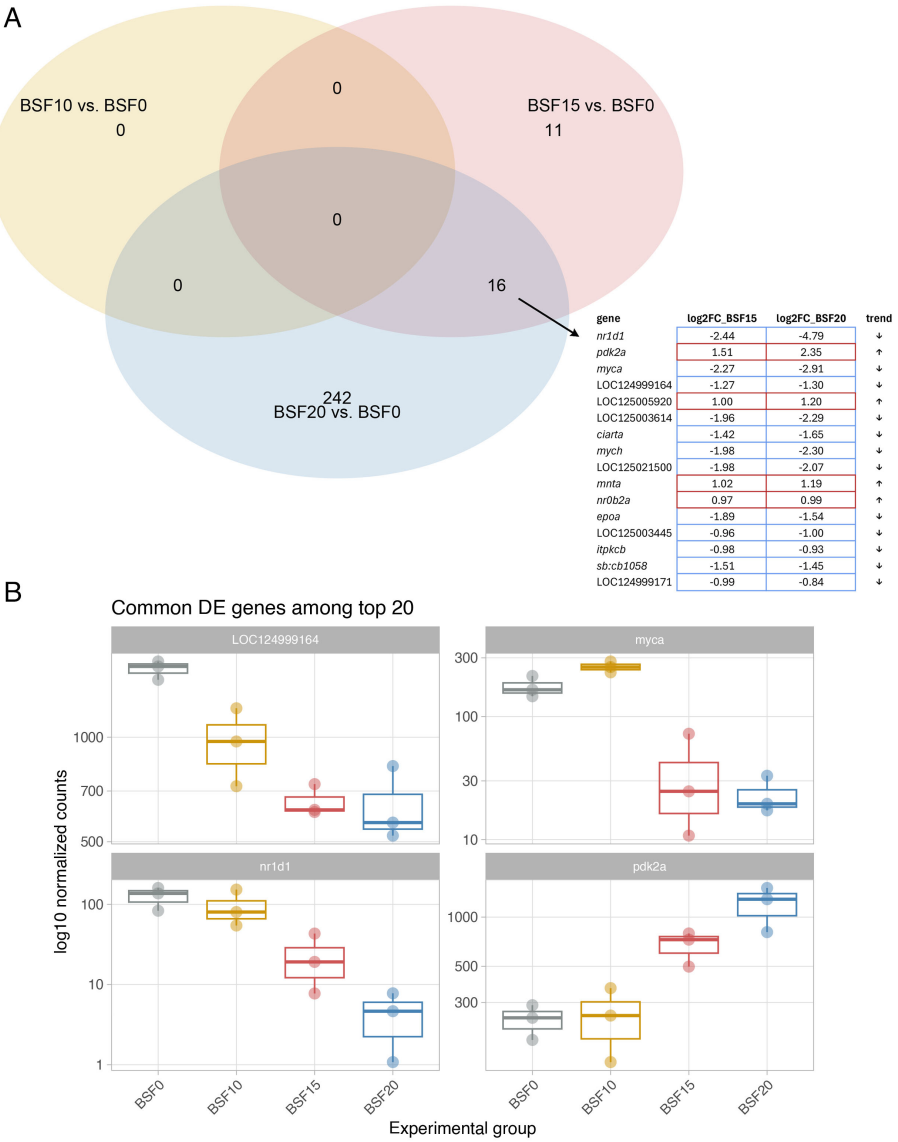

FIGURE 2
Differentially expressed (DE) genes across BSF dietary treatment groups and expression profiles of shared top DE genes. **(a)** Venn diagram illustrates the overlap of significantly DE genes identified in the three pairwise comparisons relative to the control group (BSF0). **(b)** Box plots displaying $\log_{10}$-normalized counts for the genes found among the top 20 DE genes, based on *p*-adjusted criterion, shared between BSF15 and BSF20 experimental groups.

and macrophage activation, respectively), lipid remodeling (e.g., *pnpla3* and *ldlra* reduce lipid droplets and cholesterol uptake, respectively) (Cao et al., 2022; Romeo and Valenti, 2025), thyroid hormone activation/homeostasis (*dio2*), MYC-driven proliferation (*myca* and *mych*), and circadian control (*nr1d1*). In contrast, cluster 2 grouped 117 genes displaying progressive transcriptional upregulation along increasing BSF replacement levels. Key genes here included *pdk2a*, *clockb*, *nr0b2a*, *pparaa*, *ppardb*, *acacb*, *cpt1b*, *insig1*, and *angptl4*. This cluster appeared to reflect a hepatic metabolic shift toward lipid oxidation and FA catabolism: *acacb* and *cpt1b* promote FA oxidation; *nr0b2a* and *pparaa* regulate bile acid metabolism and lipid metabolism, specifically FA uptake, mitochondrial/peroxisomal-oxidation, and ketogenesis, controlling hepatocyte gene regulatory networks; the co-induction of *clockb* alongside *nr0b2a* may reflect the disruption of *nr1d1* in Group 3 and, together, these suggest the remodeling of the hepatic circadian–metabolic axis.

The remaining clusters revealed peculiar expression patterns. For instance, group 1 exhibited a biphasic pattern of 25 genes (e.g., *eif5* —eukaryotic translation initiation factor 5 —and *igfbp2a* —insulin-like growth factor binding protein 2a, i.e., a key regulator of the IGF-1 axis central to hepatic growth control) possibly sensitive to diet composition in a threshold-independent way. An opposite transcriptional pattern was depicted in group 8, which clustered 14 genes exhibiting increasing expression at 10% and 15% dietary BSF and reversal at 20% BSF inclusion. Notable genes in this group were *elovl6* (ELOVL fatty acid elongase 6), *sptlc2b* (serine palmitoyl transferase, long chain base subunit 2b), *tcn2* (transcobalamin 2, a secreted cobalamin-binding protein that mediates the transport of vitamin B12 into cells), and *hspa5* (heat shock protein 5), an

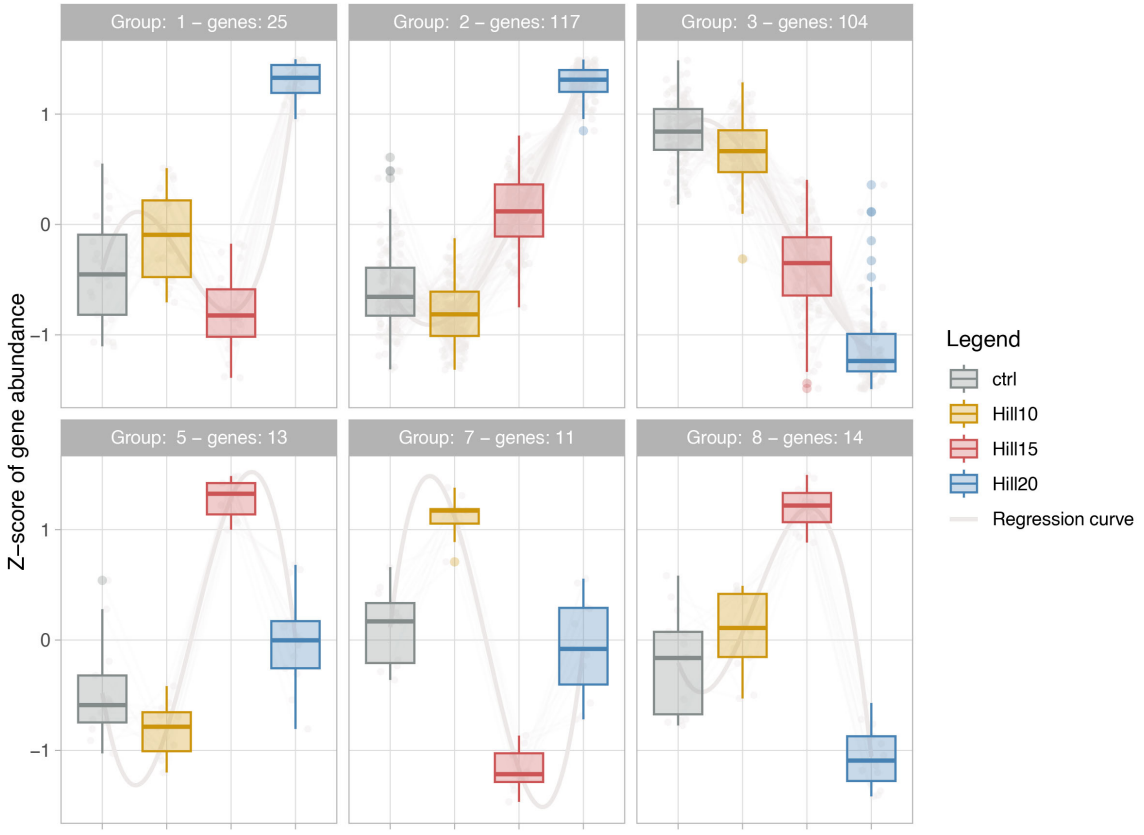

FIGURE 3
Six-group clustering of *Z*-score-transformed gene expression patterns across experimental groups resulting from the Likelihood Ratio Test investigating the goodness of fit of a reduced linear model.

endoplasmic reticulum (ER) stress chaperone involved in lipid metabolism regulation (Rehati et al., 2023). Such a pattern may represent an adaptive lipid metabolism-related remodeling response that appears stimulated at the two lowest replacement levels but overwhelmed at the highest one. Group 5 encompassed genes that share roles in cell cycle regulation, protein folding, tumor suppression, intracellular trafficking, and cell migration. Group 7 clustered genes exhibiting an early, low-dose transcriptional response consisting of an upregulation only at BSF10, followed by a strong reversal at BSF15 and a near-baseline recovery at BSF20. Four out of 11 genes included therein are not characterized (i.e., LOC125004311, LOC125018378, LOC125005863, and LOC125012174), but homology searches identified their products as microfibril-associated glycoprotein 4-like, transmembrane protein 229B-like, UDP-glucuronosyltransferase 2C1-like, and D-amino-acid oxidase-like, respectively, suggesting the occurrence of detoxification of both xenobiotics and endogenous metabolic waste. Among the remaining were *si:dkey-190g11.3* (predicted to be involved in regulation of mitochondrial ATP synthesis coupled proton transport), *npdc1a* (neural proliferation, differentiation and control 1a, whose expression increases when neural cells stop dividing and begin terminal differentiation, therefore acting as a regulator of neural cell proliferation), and *eif4ebp3l* (eukaryotic translation initiation factor 4E-binding protein 3-like, a negative regulator of translation). We can generally conclude that the liver of *M. cephalus* responded to BSF meal in a dose-structured, multimodal fashion (i.e., progressive upregulation, progressive downregulation, biphasic, and early response), as per the LRT clustering results. The two largest gene clusters appeared to define the core dose-dependent hepatic adaptation, while the small transient clusters captured threshold and early-warning signals that would be otherwise entirely missed by simple pairwise comparisons. This makes the LRT approach particularly powerful for detecting subtle but consistent patterns across ordered treatments.

To capture coordinated shifts across entire gene sets, including genes that did not individually reach DE significance, GSEA was run on the full transcriptome data, ranked by $\log_2$FC in BSF10, BSF15, and BSF20 vs. the reference group (BSF0), using KEGG pathway resources. Such an approach is more sensitive and biologically informative for gradient experiments than over-representation analysis (ORA) (Ziemann et al., 2024) because GSEA can detect pathways where genes are subtly regulated across the entire set and is not limited by arbitrary thresholds used to define input lists and statistical assumptions such as gene independence, which rarely holds true (NCI, 2023). Overall, the experimental diets significantly modulated 50 unique KEGG pathways, 40 of which are only in the BSF10 vs. BSF0 pairwise comparison (Table 2; Supplementary Table S3). Across the three contrasts, 40, 11, and 14 KEGG pathways were significant at p.adjust < 0.05, respectively.

The only gene sets modulated by all three contrasts was "mcep00190: Oxidative phosphorylation". Its NES was greatest in the BSF10 vs. BSF0 comparison (2.26, q-value 8.01E−08), with a

10.3389/fmars.2026.1901130

TABLE 2 Gene set enrichment analysis results per contrast, showing the KEGG pathways positively enriched (i.e., NES > 0) in BSF-fed samples (BSF10, BSF15, and BSF20) compared to control (BSF0).

Group	Description	Set size	NES	*p* adjusted	*q*-value
BSF10 vs. BSF0	Phagosome	171	1.47	0.021847207	0.014573719
	Peroxisome	84	1.50	0.045654434	0.030454916
	Glycolisis/Gluconeogenesis	71	1.59	0.039639285	0.026442363
	Alanine, aspartate, and glutamate metabolism	40	1.60	0.037251499	0.024849531
	Nucleotide excision repair	53	1.60	0.037251499	0.024849531
	Carbon metabolism	132	1.62	0.011302078	0.00753933
	Aminoacyl-tRNA biosynthesis	43	1.62	0.049060251	0.03272685
	Drug metabolism	46	1.68	0.032434117	0.021635978
	Primary bile acid biosynthesis	16	1.70	0.04204447	0.028046801
	Intestinal immune network for IgA production	22	1.71	0.048779612	0.032539643
	DNA replication	32	1.77	0.017654042	0.011776564
	Metabolism of xenobiotics by cytochrome P450	49	1.79	0.010545134	0.007034392
	2-Oxocarboxylic acid metabolism	39	1.81	0.010545134	0.007034392
	Biosynthesis of cofactors	155	1.82	0.000114873	7.66291E−05
	Base excision repair	45	1.83	0.006162822	0.004111062
	Pentose and glucuronate interconversions	37	1.84	0.010545134	0.007034392
	Proteasome	49	1.90	0.003074523	0.002050937
	Ascorbate and aldarate metabolism	31	1.95	0.00308212	0.002056004
	Nucleotide metabolism	93	1.99	0.000114873	7.66291E−05
	Drug metabolism	67	2.03	0.000363271	0.000242329
	Pyrimidine metabolism	62	2.06	0.000242228	0.000161584
	Steroid hormone synthesis	42	2.08	0.000287574	0.000191834
	Glutathione metabolism	60	2.08	0.000104607	6.97805E−05
	Spliceosome	143	2.08	4.35495E−06	2.90508E−06
	Oxidative phosphorylation	110	2.26	1.202E−07	8.01822E−08
	Ribosome	132	2.30	4.52992E−08	3.0218E−08
BSF15 vs. BSF0	Tight junction	184	1.54	0.014881875	0.013466517
	Salmonella infection	256	1.54	0.006862317	0.006209668
	Bacterial invasion of epithelial cells	95	1.64	0.035118196	0.031778238
	Motor proteins	114	1.64	0.035118196	0.031778238
	Phagosome	138	1.75	0.003870079	0.00350201
	Various type of N-glycan biosynthesis	40	1.83	0.040464038	0.036615658
	Oxidative phosphorylation	109	1.83	0.002337482	0.002115173
	Protein processing in endoplasmic reticulum	171	1.95	2.54818E−05	2.30584E−05
	N-Glycan biosynthesis	51	1.98	0.002337482	0.002115173
	Proteasome	48	2.43	1.30173E−07	1.17793E−07
BSF20 vs. BSF0	Glutathione metabolism	48	1.68	0.048614607	0.041248757
	Base excision repair	24	1.77	0.049922319	0.042358331
	Metabolism of xenobiotics by cytochrome P450	42	1.79	0.017678884	0.015000265

(Continued)

TABLE 2 Continued

Group	Description	Set size	NES	*p* adjusted	*q*-value
	Oxidative phosphorylation	106	1.79	0.004511568	0.003827997
	Drug metabolism	41	1.82	0.016371986	0.013891382
	Autophagy	30	1.87	0.030052976	0.025499495
	Ribosome	130	2.35	1.65E−08	0.000000014

Full results are available in Supplementary Table S3.

large log_2FC distribution of core enrichment genes (Supplementary Figure S1), and similar between contrasts BSF15/BSF20 vs. BSF0 (1.83 and 1.79, respectively) (Figure 4).

This gene set belongs to a large cluster of energy metabolism-related pathways that appeared modulated exclusively by BSF10: "Glycolysis/Gluconeogenesis" (+1.59), "Carbon metabolism" (+1.62), "2-Oxocarboxylic acid metabolism" (+1.81), "Biosynthesis of cofactors" (+1.82), and "Nucleotide/Pyrimidine metabolism" (+2.06/+2.06). These are all interconnected metabolic processes (Figure 5) that aim at utilizing and converting carbon compounds, particularly carbohydrates, into various biomolecules essential for the cell's growth, energy production, and maintenance. The persistent enrichment of oxidative phosphorylation across all replacement levels, combined with the dose-dependent upregulation of *pdk2a* (inhibiting pyruvate dehydrogenase) and *cpt1b* (FA transport into mitochondria), may indicate a metabolic switch from glycolytic flux toward oxidative FA catabolism, as BSF meal, which is rich in saturated medium-chain FA s (Toral et al., 2025), increasingly replaces FM. This appears to be a cross-species response: the coordinated transcriptional upregulation trend of FA oxidation genes (e.g., *pdk2a*, *cpt1b*, *pparaa*, and *acacb*) and persistent enrichment of oxidative phosphorylation observed in this study is confirmed in liver of largemouth bass (*Micropterus salmoides*) fed diets in which 40% of dietary FM was replaced with BSF meal (Sun et al., 2024). Integrated transcriptomic–metabolomic analyses revealed propanoate metabolism and alpha-linolenic acid metabolism, both interconnected with FA oxidation, as among the most enriched pathways.

Translation- and protein quality control-related pathways were found positively enriched across BSF replacement levels. The "Ribosome" (+2.30 at BSF10, + 2.35 at BSF20) and "Proteasome" pathways (+1.90 at BSF10, + 2.44 at BSF15) displayed greatest statistical confidence. "Spliceosome" (+2.08) and "Aminoacyl −tRNA biosynthesis" (+1.62) were only enriched in fish receiving the BSF10 diet, "Protein processing in endoplasmic reticulum" and "N-Glycan biosynthesis" (+1.98 and +1.95, respectively) were exclusively enriched by BSF15, while "Autophagy" was notably the only positively enriched pathway exclusively modulated by BSF20 (Figure 4; Supplementary Table S3). Together, these results are consistent with an upregulation of the entire cascade from mRNA processing (spliceosome), tRNA charging, ribosome-mediated translation, ER-based folding, and glycosylation to proteasomal clearance of misfolded proteins. The lowest dietary BSF inclusion stimulated hepatic protein synthesis, while increasing BSF percentages required extensive folding, glycosylation, and stability, up to the point of degrading and recycling damaged organelles and misfolded proteins into amino acids, supposedly in an attempt of maintaining cellular homeostasis under stressful circumstances (Chun and Kim, 2018). The upregulation of ER stress-related genes (Figure 3; Supplementary Table S2) as well as the enrichment in the biosynthetic pathway of N-glycan is likely a compensatory response to impaired ER function, because of its critical role in ensuring protein function (i.e., folding, trafficking, stability, and interaction) (Esmail and Manolson, 2021). From a fish physiology standpoint, this is consistent with a liver metabolism that responds to a nutritionally distinct protein source by upregulating the entire machinery of protein processing. The induction of ER stress and protein quality control machinery herein observed aligns closely with findings in largemouth bass fed 40% FM replacement with BSF meal, where upregulated genes were significantly enriched in protein catabolism, ER stress (*hspa5* and *hsp90b1*), and N-glycosylation processes (Sun et al., 2024) (a 20% replacement was tested but not investigated via RNA-seq). Notably, while ER stress co-occurred with measurable growth impairment in largemouth bass, a non-significant growth suppression was detected in *M. cephalus* fed BSF meal-based diets, up to 20% of FM replacement (Randazzo et al., 2026). The induction of ER stress and impaired phospholipid metabolism was also reported in juvenile Pacific white shrimp (*Litopenaeus vannamei*) fed on a low FM formulation (Xie et al., 2020).

"Glutathione metabolism" (+2.08 and +1.68), Metabolism of xenobiotics by cytochrome P450 (+1.79 and +1.78), and Drug metabolism (+2.03 and +1.82) were consistently enriched by BSF10 and BSF20 diets. This pattern seems to indicate that even at low insect meal inclusion, the liver mounts phase I/II detoxification and antioxidant defenses, likely in response to BSF bioactive compounds (e.g., chitin-derived products, lauric acid, and antimicrobial peptides), in a particularly robust manner at the lowest (10%) and highest (20%) replacement levels, with a temporary attenuation at BSF15. This result strongly agrees with the clustered transcriptional signatures of genes included in Group 7 (Figure 3).

A characteristic pattern can be drawn from the bottom segment of Figure 4, which displays a block of pathways almost exclusively suppressed in the BSF10 and BSF20 groups. The large majority of those gene sets are signaling, hormone, and receptor pathways. Among the 10 most suppressed pathways in BSF10, 8 (i.e., MAPK, GnRH, FoxO, Hormone, ErbB, Calcium, Apelin, and Insulin signaling pathways) fall within such a functional category, with NESs ranging from −1.69 (MAPK) to −1.48 (Insulin). While the suppression of these two pathways is congruent with LRT Cluster 3 downregulation of *myca*, *igf2b*, *pik3r1* (Phosphoinositide-3-Kinase Regulatory Subunit 1), and *socs3b*, the detected trend overall indicates reduced hepatic growth factor and nutrient-sensing cascades, reasonably in response to the altered amino acid and lipid

FIGURE 4
Gene set enrichment analysis (GSEA) results across dietary BSF meal inclusion levels. Dot plot summarizing the significantly enriched KEGG pathways (adjusted *p*-value < 0.05) identified by GSEA in pairwise comparisons of each BSF-supplemented dietary group against the control diet (BSF10/15/20 vs. BSF0). Each dot represents a significantly enriched pathway in at least one contrast. Dot size is proportional to statistical significance, with larger dots indicating lower adjusted *p*-values (FDR-corrected), as shown in the legend (ranging from 0.04992 to 1.65×10^{-8}). Dot color reflects the Normalized Enrichment Score (NES): red/warm tones indicate positive enrichment (NES > 0; pathway genes predominantly upregulated relative to BSF0), while green/cool tones indicate negative enrichment (NES < 0; pathway genes predominantly downregulated relative to BSF0), with the color scale ranging from −2 to +2. Pathways are listed on the *y*-axis by their KEGG identifier and name. Only pathways reaching statistical significance (FDR < 0.05) in at least one contrast are shown; the absence of a dot for a given pathway–contrast combination indicates non-significant enrichment.

profile of insect meal-based diets. A suppression in signaling cascades (i.e., regulation of cell population proliferation, TOR signaling, p53 signaling pathway, regulation of MAPK cascade, and RIG-I-like receptor signaling pathway) was seen in the phylogenetically distant *M. salmoides* at 40% FM replacement (Sun et al., 2024). A further convergent signature between *M. salmoides* and *M. cephalus* feeding on alternative insect ingredients was the impact on circadian rhythm regulation, with *nr1d1* as master transcriptional repressor linking circadian timing to hepatic lipid, bile acid, and glucose metabolism identified among the most downregulated genes. This is striking, considering their distinct biology, habitat, phylogeny (Subseries Eupercaria, Order Perciformes vs. Subseries Ovalentaria, Order Mugiliformes) and estimated time of divergence of 150–80 MYA (Near et al., 2012; Liu et al., 2025).

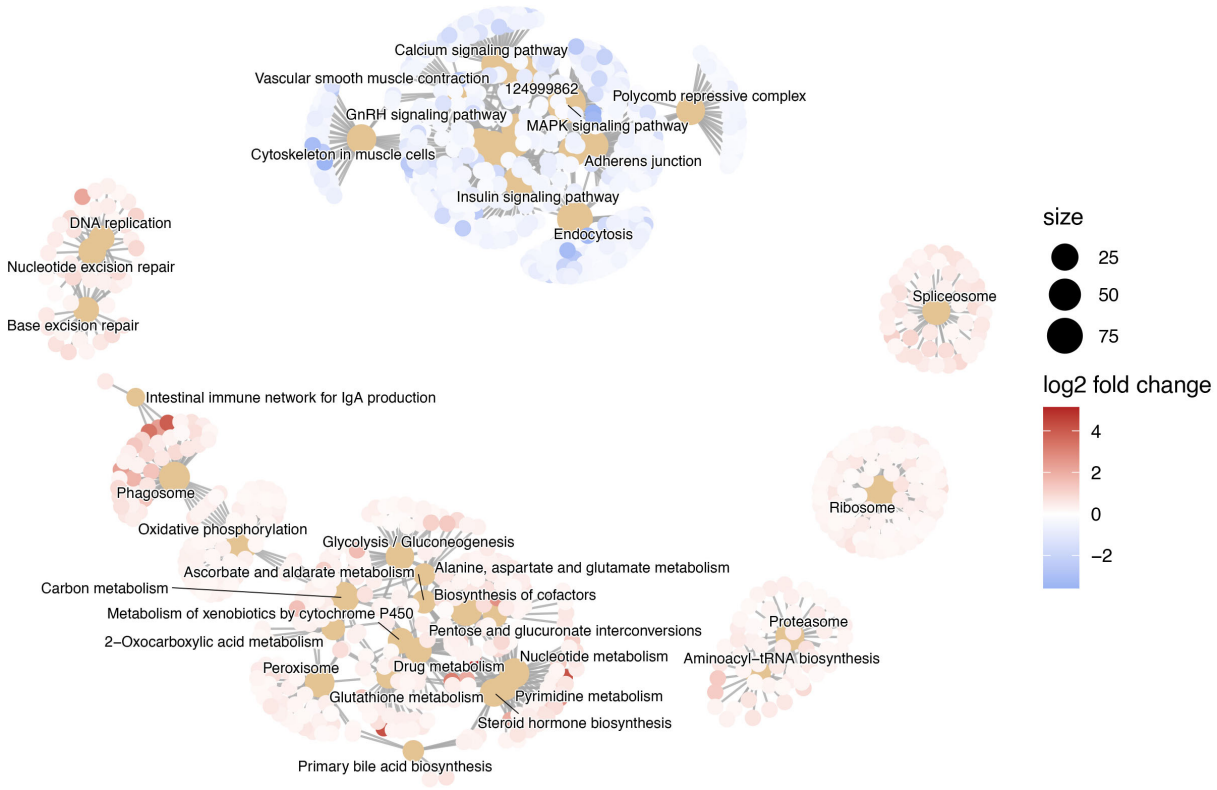

FIGURE 5
Effect size-annotated gene category network plot showing the linkage of core enrichment genes across enriched pathways in BSF10 vs. BSF0 comparison. Node size is proportional to gene abundance.

"Cytoskeleton in muscle cells" (−2.04) was the single most suppressed pathway at 20% BSF replacement (*q*-value 3.13E−06), followed by "Focal adhesion" (−1.76) and "Regulation of actin cytoskeleton" (−1.49). This prominent cytoskeletal suppression at the highest inclusion levels may reflect altered hepatic tissue architecture or reduced cellular remodeling capacity that may hinder liver structural integrity.

While the "Ribosome" gene set (i.e., structural component) is enriched, "Ribosome biogenesis in eukaryotes" (i.e., the upstream assembly machinery) is suppressed at BSF15 only with a NES of −1.96 accounting for the most negative score in the whole dataset (Supplementary Figure S2). Such a dissociation between ribosome use and ribosome production in this experimental group may indicate a transitional stress state where existing ribosomes are more active, but new ribosome assembly is temporarily repressed. That would be consistent with the ER stress signal (*hspa5*) identified by the LRT Cluster 8. In a previous study (Randazzo et al., 2026), no hepatic histological alteration was highlighted in *M. cephalus* fed with BSF-based diets over the same period as the present study (138 days); thus, the results herein obtained could represent molecular pathways that require longer time to be histologically appreciable.

Research aimed at integrating or replacing FM with insect meal in aquaculture feeds have flourished in the last decade, encouraged by the urgent need of enhancing long-term sustainability of the sector. However, the vast majority of studies focused on determining fish welfare parameters, variations in growth indices, status of intestinal health and digestive enzymatic activity, fillet quality, or, more recently, changes in the gut microbiota (e.g., Costa et al., 2026; Oteri et al., 2026; Varga et al., 2026; Drosdowech et al., 2024; Rimoldi et al., 2024; Hasan et al., 2023; Basili et al., 2025). Even when transcriptomics was considered, gene expression data often relied on targeted qPCR assays of select candidate genes (e.g., Borland et al., 2024; Sankappa et al., 2024). While such an approach may aid in resolving specific pathways of interest, it inherently excludes the investigation of unforeseen and/or novel responses, such as the circadian–metabolic axis remodeling identified here.

3.2 Fatty acid composition of diets and fish fillets

3.2.1 Diets

In Table 3, the proximate composition and the FA profile of the experimental diets are reported. The experimental diets resulted in approximately isoproteic and isolipidic content. In particular, protein content ranged from 37.2% in the BSF0 diet to 36.5% in the BSF20 diet; lipid content, in terms of ether extract, ranged from 9.1% to 9.8% in BSF0 and BSF20 diets, respectively. In this study, the FA composition of the final mixture of the experimental diets was analyzed with the practical aim of correlating the effect of the diet on the transcriptomic response of the liver and the FA composition of the fillet. According to our analyses, the lipid fraction composition significantly differed among the diets. Among SFAs, palmitic acid (C16:0) was the most represented,

with minor changes within the diets, accounting for 10.85%, 11.27%, 11.11%, and 11.3% in BSF0, BSF10, BSF15, and BSF20, respectively. Notably, lauric acid was very low in the reference BSF0 diet (0.05%), while proportionally increased with BSF inclusion, accounting for 1.88%, 2.78%, and 3.62% of the total FAMEs in the BSF10, BSF15, and BSF20 diets, respectively. A comparable but less pronounced pattern emerged for myristic acid (C14:0), which rose from 2.06% in BSF0 to 2.41%, 2.48%, and 2.58% in BSF10, BSF15, and BSF20, respectively, indicating a progressive increase in its dietary proportion alongside higher levels of BSF meal inclusion. Minor percentages of pentadecanoic (C15:0), heptadecanoic (C17:0), stearic (C18:0), arachidic (C20:0), behenic (C22:0), tricosanoic (C23:0), and lignoceric (C24:0) acids were also detected at comparable levels across all four diet formulations. These results linearly reflected the FA features of the ingredients used as protein sources in the diets, particularly regarding lauric acid. Lauric acid is recognized as an antibacterial, antifungal, antiviral, and antitumoral agent (Borrelli et al., 2021; Herdiyati et al., 2021; Akula et al., 2021; Lappano et al., 2017), and represents a distinctive trait of BSF meal, ranging from 37% to 67% of total FAs, depending on the insect developmental stage and on the rearing substrate (Ramos-Bueno et al., 2016); in BSF prepupae, i.e., the larval stage used herein in the diets, lauric acid may account for approximately 52% of the total FAs (Ewald et al., 2020; Almeida et al., 2020; Suryati et al., 2023). As regards monounsaturated fatty acids (MUFAs), oleic acid (C18:1n9c) was the most represented in all the diets, accounting for 23.86%, 24.32%, 23.97%, and 23.75%, followed by palmitoleic acid (C16:1), which accounted for 3.82%, 3.91%, 3.77%, and 3.70% in BSF0, BSF10, BSF15, and BSF20, respectively.

A small percentage of erucic acid (C22:1n9) was detected in the BSF0 diet (1.22%), while but almost totally disappeared in the other diets. Erucic acid is typically present at high concentrations in the seeds from Brassicaceae plant genus, while in other feed stuff, including insect meal, it can occasionally occur in trace amounts (Ackman, 2008; Sissener et al., 2018; IJdema et al., 2025).

As regards the most represented PUFAs, EPA (20:5n3) accounted for 4.03%, 3.94%, 3.85%, and 3.78% and DHA (22:6n3) accounted for the 4.12%, 4.04%, 4.06%, and 4.05% in the BSF0, BSF10, BSF15, and BSF20 diets, respectively. EPA and DHA are important FAs abundantly present in marine-derived feed ingredients including FM (Cho and Kim, 2011), and their decrease was expected, as BSF meal gradually replaced FM in the reference diet. However, the low basal FM content (3 g 100 g^{-1}) of the BSF0 diet and the consequent low replacement (−1.2, −1.8, and −2.4 g 100 g^{-1} in the BSF-based diets) lead to marginal reduction in EPA and DHA levels and to an overall comparable total n3 FAs content among diets. The low amount of FM in the reference BSF0 diet was established based on the low dietary requirement of this ingredient for *M. cephalus*, as previously shown (Bertini et al., 2023), which is one of the ecologically relevant advantages of farming this fish species.

3.2.2 Fillets

In Table 4, the proximate composition and the FA profile of the fish fillets are reported for each dietary group. Samples showed a comparable proximate composition, regardless of the diet used, showing protein contents of 66.15% ± 0.83%, 68.15% ± 0.38%, 66.93% ± 1.92%, and 68.41% ± 2.45%, and lipid contents of 22.59% ± 1.37%, 23.06% ± 0.80%, 21.00% ± 1.13%, and 20.60% ± 0.97% in BSF0, BSF10, BSF15, and BSF20 groups, respectively. These results indicate that replacing protein sources (FM, PM, FtM, and SBM) of the reference diet with BSF meal did not significantly affect protein and lipid content of the final edible product and that the BSF percentages used in the present study are well tolerated by *M. cephalus*, as previously observed also under a strictly zootechnical point of view (Randazzo et al., 2026).

Nevertheless, dietary BSF meal resulted in different fillet lipid profiles across the groups. In particular, among SFAs, lauric acid (C12:0) content linearly reflected the diets composition, with statistically significant higher percentages ($p < 0.0001$) in fillets from BSF10, BSF15, and BSF20 groups (0.73% ± 0.12%, 1.14% ± 0.16%, and 1.39% ± 0.13%, respectively) compared to the BSF0 ones (0.08% ± 0.01%). However, the most quantitatively represented SFA in all experimental groups was the palmitic acid (C16:0), regardless of the diet used. Palmitic acid gradually decreased across BSF treatments, with statistically significant lower values ($p = 0.0405$) in BSF20 (19.92% ± 0.37%) compared to the other groups (21.05% ± 0.32%, 21.79% ± 0.58%, and 20.45% ± 1.07% in BSF0, BSF10, and BSF15, respectively). Despite the fact that dietary palmitic acid content slightly increased in BSF10, BSF15, and BSF20 diets (Table 3), the inverse effect on fillet composition observed in our study partially agrees with previous research. This inverse relation in diet/fillet palmitic content acid was previously observed in gilthead seabream (*Sparus aurata*) fed with increased levels of BSF meal and was attributed to the activation of FA elongation pathways that resulted in a parallel increase in stearic acid (C18:0) percentages in fillets (Moutinho et al., 2024). In our study, while no statistically significant differences were observed in fillet stearic acid content across the experimental groups, a similar trend was observed in heptadecenoic acid (17:0) content, particularly in fish fed the BSF20 diet that were slightly but significantly higher (0.25% ± 0.01%) compared to the other groups (0.23% ± 0.01%, 0.21% ± 0.02%, and 0.23% ± 0.02%, in BSF0, BSF10, and BSF15 groups, respectively). This result suggests that FA elongation processes could occur in *M. cephalus*, as also supported by the increased hepatic expression of the fatty acid elongase 6 transcripts in the BSF20 group. However, our results are in contrast with a trend observed in the zebrafish (*Danio rerio*) model, in which increased dietary BSF meal resulted in increased palmitic acid in fish (Zarantoniello et al., 2021; Truzzi et al., 2023), which is consistent with the different ability in converting shorter precursors to longer-chain FAs between freshwater and marine fish species (Monroig and Kabeya, 2018).

As regards unsaturated FAs, palmitoleic acid (C16:1), oleic acid (C18:1n9), and the n6 linoleic (C18:2n6c), representing important components of *M. cephalus* lipid composition (Argyropoulou et al., 1992; Şengör et al., 2003; Özogul and Özogul, 2007; Ramos-Júdez et al., 2023), were the most represented in fillets from all the groups and did not differ across dietary treatments. The slight, even if not statistically significant, increase of alpha linolenic acid (C18:3n3) in fillets from the BSF20 group reflects the trend in the dietary content of this FA, and it is also consistent with findings from the integrated transcriptomic–metabolomic analyses that highlighted enrichment in the pathways

10.3389/fmars.2026.1901130

TABLE 3 Proximate composition and fatty acid composition of the experimental diets.

	BSF0	BSF10	BSF15	BSF20
Proximate composition				
Protein ($n \times 6.25$, %)	37.2	36.9	36.6	36.5
Lipids (%)	9.1	9.5	9.7	9.8
Ash (%)	6.7	6.8	6.6	6.5
Fatty acids				
C04:0 - Butyric	ND	ND	ND	ND
C06:0 - Capronic	ND	ND	ND	ND
C08:0 - Caprilic	ND	ND	ND	ND
C10:0 - Caprinic	ND	ND	ND	ND
C11:0 - Undecanoic	ND	ND	ND	ND
C12:0 - Lauric	0.05	1.88	2.78	3.62
C14:0 - Myristic	2.06	2.41	2.48	2.58
C14:1 - Myristoleic	0.06	0.07	0.07	0.07
C15:0 - Pentadecanoic	0.16	0.18	0.18	0.18
C15:1 - Pentadecenoic (cis-10)	0.01	0.01	0.01	0.01
C16:0 - Palmitic	10.85	11.27	11.11	11.03
C16:1 - Palmitoleic	3.82	3.91	3.77	3.70
C17:0 - Heptadecanoic	0.15	0.16	0.16	0.15
C17:1 - Heptadecenoic (cis-10)	0.20	0.15	0.18	0.17
C18:0 - Stearic	3.56	3.61	3.55	3.50
C18:1n9t - Trans oleic	0.07	0.08	0.07	0.07
C18:1n9c - Oleic	23.86	24.32	23.97	23.75
C18:2n6t - Trans linoleic	0.09	0.10	0.07	0.09
C18:2n6c - Linoleic	35.5	36.18	36.08	35.69
C20:0 - Arachidic	0.23	0.23	0.23	0.23
C18:3n6 - Gamma linolenic	0.07	0.06	0.06	0.06
C20:1 - Eicosenoic (cis-11)	4.25	4.39	4.31	4.27
C18:3n3 - Alpha linolenic	1.04	1.16	1.17	1.18
C21:0 - Eneicosanoic	ND	ND	ND	ND
C20:2n6 - Eicosadienoic (cis-11.14)	0.20	0.20	0.19	0.19
C22:0 - Behenic	0.43	0.43	0.43	0.43
C20:3n6 - Eicosatrienoic (cis-8.11.14)	0.05	0.05	0.04	0.04
C22:1n9 - Erucic	1.22	0.38	0.37	0.36
C20:3n3 - Eicosatrienoic (cis-11.14.17)	0.10	0.11	0.11	0.11
C20:4n6 - Arachidonic	0.06	0.28	0.27	0.26
C23:0 - Tricosanoic	0.31	0.08	0.08	0.08
C22:2n6 -Docosadienoic (cis-13.16)	0.04	0.04	0.04	0.04
C24:0 - Lignoceric	0.14	0.13	0.14	0.14
C20:5n3 -Eicosapentaenoic (cis-5.8.11.14.17) (epa)	4.03	3.94	3.85	3.78
C24:1 - Tetracosenoic (nervonic)	0.21	0.23	0.21	0.21

(Continued)

10.3389/fmars.2026.1901130

TABLE 3 Continued

	BSF0	BSF10	BSF15	BSF20
Fatty acids				
C22:6n3 - Docosahexaenoic (cis-4.7.10.13.16.19) (dha)	4.12	4.04	4.06	4.05
Trans fatty acids isomers				
C18:1 - (Elaidinic)	0.090	0.08	0.07	0.08
C18:2 + c18:3	0.091	0.10	0.07	0.09
n3	9.29	9.18	9.12	9.06
n6	35.77	36.47	36.34	35.96
n9	28.17	24.77	24.41	24.19

ND, not detected.

involved in alpha-linolenic acid metabolism, particularly at high dietary BSF meal inclusion. Moreover, in our study, statistically significant (p = 0.0169) higher percentages of the trans linoleic acid (C18:2n6t) were detected in the BSF10 group (1.12% ± 0.22%) compared to all the other dietary groups where it accounted for the 0.88% ± 0.08% 0.78% ± 0.17%, and 0.62% ± 0.05% in groups BSF0, BSF15, and BSF20, respectively. Trans linoleic acid trans isoform represents a rare isomer of the linoleic acid, ascribable to the class of conjugated linoleic acids (CLAs), which is normally found as a minor constituent in the lipid fraction of many kinds of feedstuff, including animal fat, and also found in insect meal (Goncalves et al., 2010; Carpentier et al., 2024). Although trans FA isomers are generally considered harmful for human health, CLAs are considered safe and even beneficial when consumed in low amounts (Dhiman et al., 1999; Gaullier et al., 2002, 2005; Desroches et al., 2005; Basak and Duttaroy, 2020). Moreover, CLA may play a species-specific role in decreasing fish SFAs and MUFAs, which also shows a marketable additional value (Choi et al., 1999; Twibell et al., 2000; Diez et al., 2007). In addition, in the BSF10 group, a trending decrease in the percentages of erucic acid (C22:1n9), eicosatrienoic acid (C20:3n3), and tricosanoic acid (C23:0) was observed compared to the other groups. However, the overall low amount of the above FAs in fillets (Table 4) makes them negligible from a marketable perspective. Notably, a significant increase (p = 0.0383) in n3 FAs in fillets from the BSF20 group (9.10% ± 0.42%) was observed compared to all the other groups (7.82% ± 0.81%, 6.86% ± 0.86%, and 7.34% ± 0.26% in BSF0, BSF10, and BSF15, respectively). Among n3, DHA (22:6n3) levels were significantly higher (p = 0.0436) in fillets from the BSF20 group (5.32% ± 0.28%) compared to those from all the other groups (4.40% ± 0.22%, 3.70% ± 0.27%, and 4.16% ± 0.19% in BSF0, BSF10, and BSF15 groups respectively). A predominance of n6 FAs over n3 ones had been expected as BSF percentage increased in the diet. The resulting shift in n3/n6 ratio in BSF-based diets, particularly in the BSF20 group, may have had a role in stimulating conversion mechanisms able to trigger the endogenous production of n3-PUFAs.

Moreover, a parallel statistically significant increase in erucic acid (C22:1n9), eicosatrienoic acid (C20:3n3), and tricosanoic acid (C23:0) in fillet from fish fed BSF20 diet could be a consequence of the activation of conversion mechanisms acting on C18 PUFA to obtain longer C20 and C22 homologues. Compared to freshwater species, marine fish generally retain a reduced ability of converting shorter precursors to longer-chain FAs, although this is influenced by the dietary lipid source and does not represent a fixed condition (Sargent et al., 2002). For instance, in tilapia (*Oreochromis niloticus*), a freshwater species known to possess some ability to elongate and desaturate C18:3n-3 to C20:5n-3 and C22:6n-3 (Olsen et al., 1990; Tocher, 2003), the efficiency in the conversion of C18:3n-3 to longer-chain n-3 PUFA derivatives depends on dietary lipid sources and on experimental conditions (Karapanagiotidis et al., 2007).

Even if lipid metabolism has been almost totally unexplored in *M. cephalus* (Kelly et al., 1958; Ramos-Júdez et al., 2023), the capability to adapt to low dietary PUFAs has been established for freshwater and euryhaline fish species (Tocher et al., 2001, 2003; Carvalho et al., 2022). For instance, low FM diets were shown to induce the elongase and desaturase enzymatic pathways in gilthead seabream (Pulido-Rodriguez et al., 2021). Historic studies hypothesized that *M. cephalus* can convert dienoic acids (i.e., C20:2n6 and C20:3n6) in tetraenoic, pentaenoic, and hexaenoic acids, and reported the ability to convert linoleic acid to a trienoic acid (Kelly et al., 1958). However, more recent research conducted on strongly related fish species, including *Chelon labrosus*, *Mugil liza*, and *Liza aurata*, suggest that this fish family can be able to *de novo* synthetize long-chain FAs starting from dietary lipid sources different from fish oils (Rosas et al., 2019; Marrero et al., 2024; Quirós-Pozo et al., 2025). This also depends on the functionalization of fatty acid desaturase (FAD) enzymatic activity, responsible for adding double bonds to the carbon chains. PUFA biosynthetic ability in fish is strictly species-specific, and supposedly phylogenetically determined as a consequence of trophic level, habitat (freshwater vs. marine), and trophic ecology (Sargent et al., 2002; Stubhaug et al., 2005; Zheng et al., 2005; Castro et al., 2016).

The increase in total n3 FAs and DHA (C22:6n3) observed in fillets of the BSF20 group, despite a comparable content of these FAs within the diets with marginal reduction in BSF20 diet, suggests that *M. cephalus* engaged active hepatic lipid processing rather than passive dietary FA deposition. Two complementary transcriptomic signatures support this interpretation. First, *elovl6* (ELOVL fatty acid elongase 6), included in LRT Cluster 8, was progressively upregulated at BSF10 and BSF15 (i.e., conditions associated with moderate increases in dietary medium-chain saturated FAs) before reverting toward baseline at BSF20. This biphasic pattern is consistent with a transient enhancement of hepatic elongation capacity at intermediate BSF inclusion levels, potentially channelling C16–C18 substrates into longer-chain

10.3389/fmars.2026.1901130

TABLE 4 Fatty acid composition (expressed as percentage of total fatty acids) of the fillets from fish fed the different experimental diets.

	BSF0	BSF10	BSF15	BSF20	*p*-value
Proximate composition					
Protein ($n \times 6.25$, %)	66.15 ± 0.83	68.15 ± 0.38	66.93 ± 1.92	68.41 ± 2.45	0.3426
Lipids (%)	22.59 ± 1.37	23.06 ± 0.80	21.00 ± 1.13	20.60 ± 0.97	0.0638
Ash (%)	5.46 ± 0.13	5.47 ± 0.32	6.50 ± 0.39	5.37 ± 1.23	0.2049
Fatty acids					
C04:0 - Butyric	ND	ND	ND	ND	–
C06:0 - Capronic	ND	ND	ND	ND	-
C08:0 - Caprilic	ND	ND	ND	ND	–
C10:0 - Caprinic	ND	ND	ND	ND	-
C11:0 - Undecanoic	ND	ND	ND	ND	–
C12:0 - Lauric	**0.08 ± 0.01^{c}**	**0.73 ± 0.12^{b}**	**1.14 ± 0.16^{a}**	**1.39 ± 0.13^{a}**	**<0.0001**
C14:0 - Myristic	4.0 ± 0.44	4.38 ± 0.23	4.26 ± 0.36	4.86 ± 0.31	0.0785
C14:1 - Myristoleic	0.14 ± 0.03	0.15 ± 0.01	0.12 ± 0.01	0.14 ± 0.02	0.4229
C15:0 - Pentadecanoic	0.33 ± 0.03	0.31 ± 0.04	0.33 ± 0.05	0.39 ± 0.02	0.1025
C15:1 - Pentadecenoic (cis-10)	0.01 ± 0.0	0.01 ± 0.0	0.1 ± 0.0	0.1 ± 0.0	0.4055
C16:0 - Palmitic	**21.05 ± 0.32^{a}**	**21.79 ± 0.58^{ab}**	**20.45 ± 1.07^{ab}**	**19.92 ± 0.37^{b}**	**0.0405**
C16:1 - Palmitoleic	9.79 ± 1.02	10.07 ± 0.60	8.56 ± 0.73	8.86 ± 0.91	0.1560
C17:0 - Heptadecanoic	**0.23 ± 0.01^{b}**	**0.21 ± 0.02^{b}**	**0.23 ± 0.02^{b}**	**0.25 ± 0.01^{a}**	**0.0482**
C17:1 - Heptadecenoic (cis-10)	0.23 ± 0.05	0.21 ± 0.03	0.22 ± 0.07	0.28 ± 0.03	0.2243
C18:0 - Stearic	2.89 ± 0.15	2.88 ± 0.03	2.99 ± 0.11	2.87 ± 0.06	0.4929
C18:1n9t - Trans oleic	**0.19 ± 0.01^{b}**	**0.22 ± 0.01^{a}**	**0.21 ± 0.01^{ab}**	**0.20 ± 0.01^{ab}**	**0.0236**
C18:1n9c - Oleic	22.52 ± 0.76	22.33 ± 0.50	22.12 ± 0.45	21.50 ± 0.42	0.2038
C18:2n6t - Trans linoleic	**0.88 ± 0.08^{ab}**	**1.12 ± 0.22^{a}**	**0.78 ± 0.17^{ab}**	**0.62 ± 0.05^{b}**	**0.0169**
C18:2n6c - Linoleic	23.82 ± 1.29	23.09 ± 1.57	25.11 ± 1.92	23.56 ± 1.37	0.4701
C20:0 - Arachidic	0.29 ± 0.02	0.26 ± 0.02	0.29 ± 0.01	0.29 ± 0.02	0.1226
C18:3n6 - Gamma linolenic	0.45 ± 0.01	0.52 ± 0.06	0.47 ± 0.05	0.44 ± 0.04	0.2009
C20:1 - Eicosenoic (cis-11)	3.00 ± 0.09	2.78 ± 0.06	2.99 ± 0.13	2.95 ± 0.08	0.0683
C18:3n3 - Alpha linolenic	1.85 ± 0.10	1.85 ± 0.17	1.88 ± 0.10	2.00 ± 0.03	0.3316
C21:0 - Eneicosanoic	ND	ND	ND	ND	-
C20:2n6 - Eicosadienoic (cis-11.14)	0.84 ± 0.01	0.82 ± 0.01	0.85 ± 0.02	0.85 ± 0.03	0.2985
C22:0 - Behenic	0.14 ± 0.01	0.13 ± 0.01	0.15 ± 0.01	0.14 ± 0.01	0.1062
C20:3n6 - Eicosatrienoic (cis-8.11.14)	0.25 ± 0.02	0.26 ± 0.01	0.24 ± 0.04	0.24 ± 0.03	0.8581
C22:1n9 - Erucic	**0.27 ± 0.01^{a}**	**0.25 ± 0.01^{b}**	**0.28 ± 0.01^{a}**	**0.28 ± 0.02^{a}**	**0.0005**
C20:3n3 - Eicosatrienoic (cis-11.14.17)	**0.19 ± 0.01^{ab}**	**0.18 ± 0.01^{b}**	**0.19 ± 0.02^{ab}**	**0.22 ± 0.01^{a}**	**0.0186**
C20:4n6 - Arachidonic	0.34 ± 0.04^{ab}	0.32 ± 0.03^{b}	0.34 ± 0.02^{ab}	0.38 ± 0.01^{a}	0.1074
C23:0 - Tricosanoic	**0.08 ± 0.01^{ab}**	**0.07 ± 0.01^{b}**	**0.08 ± 0.01^{ab}**	**0.09 ± 0.01^{a}**	**0.0020**
C22:2n6 -Docosadienoic (cis-13.16)	0.10 ± 0.0	0.10 ± 0.01	0.10 ± 0.01	0.10 ± 0.0	0.3300
C24:0 - Lignoceric	0.04 ± 0.01	0.04 ± 0.01	0.13 ± 0.15	0.04 ± 0.01	0.0855

(Continued)

10.3389/fmars.2026.1901130

TABLE 4 Continued

	BSF0	BSF10	BSF15	BSF20	*p*-value
Fatty acids					
C20:5n3 -Eicosapentaenoic (cis-5.8.11.14.17) (epa)	1.82 ± 0.20	1.58 ± 0.20	1.57 ± 0.33	1.99 ± 0.12	0.1435
C24:1 - Tetracosenoic (nervonic)	0.19 ± 0.02^{ab}	0.17 ± 0.02^{b}	0.19 ± 0.01^{ab}	0.21 ± 0.02^{a}	0.1002
C22:6n3 - Docosahexaenoic (cis-4.7.10.13.16.19) (dha)	**4.40 ± 0.22^{b}**	**3.70 ± 0.27^{b}**	**4.16 ± 0.19^{b}**	**5.32 ± 0.28^{a}**	**0.0436**
Trans fatty acids isomers					
C18:1 - (Elaidinic)	0.19 ± 0.01	0.22 ± 0.01	0.21 ± 0.01	0.20 ± 0.01	0.0525
C18:2 + c18:3	**0.88 ± 0.08^{ab}**	**1.12 ± 0.22^{a}**	**0.78 ± 0.17^{ab}**	**0.62 ± 0.05^{b}**	**0.0169**
n3	**7.82 ± 0.81^{b}**	**6.86 ± 0.86^{b}**	**7.34 ± 0.26^{b}**	**9.10 ± 0.42^{a}**	**0.0383**
n6	25.27 ± 1.16	24.99 ± 1.38	26.68 ± 1.99	24.95 ± 1.40	0.4951
n9	22.98 ± 0.77	22.80 ± 0.50	22.61 ± 0.47	21.98 ± 0.41	0.2145

Values are expressed as mean ± SD. Different letters indicate statistically significant differences among the groups ($p < 0.05$). ND, not detected.
Statistically significant differences are indicated in bold.

products but overwhelmed at the highest inclusion level. Second, and arguably more explanatory of the BSF20 fillet outcome, the dose-dependent upregulation of FA oxidation genes in LRT Cluster 2, including *pdk2a*, *pparaa*, and *ppardb* (master regulators of hepatic β-oxidation), *acacb* (acetyl-coenzyme A carboxylase beta), and *cpt1b* (carnitine palmitoyl transferase 1b, enabling mitochondrial import of long-chain FAs), indicates enhanced mitochondrial oxidation of the medium-chain saturated FAs abundant in BSF meal, particularly lauric (C12:0) and palmitic (C16:0) acids. This preferential oxidation of dietary SFAs may reduce their competition with LC-PUFAs for esterification into membrane phospholipids and triglycerides destined for muscle deposition, effectively sparing and concentrating DHA in the fillet. The inverse relationship between diet and fillet palmitic acid content observed across BSF-fed groups provides additional biochemical support for this active hepatic processing. It should be noted that, in the absence of differential expression data for *fads2* (Δ6-desaturase) (Supplementary Table S1), *de novo* elongation–desaturation biosynthesis from α-linolenic acid (ALA, C18:3n3) precursors to DHA cannot be confirmed and is considered a secondary hypothesis requiring further dedicated investigation.

liver can accommodate *H. illucens* meal at up to 15% replacement without evidence of metabolic failure, though the progressive suppression of growth-factor signaling and cytoskeletal integrity at the highest level warrants attention in longer-term feeding trials.

The comparable protein and lipid content of the fillets among the treatments assures that the proximate composition of the final edible product is not impaired by dietary BSF meal. In addition, the improved FA profile of fish fillets, indicated by increased percentages of n3, in fish fed the BSF20 diet suggests that *M. cephalus* can activate elongase and desaturase processes better than strictly carnivorous marine species and, therefore, more similarly to freshwater fish species. However, further analyses, including enzymatic assays or metabolomics could better clarify this point. The low trophic level of *M. cephalus*, along with its euryhaline habits, supports its capacity to adapt to low-FM diets and its ability to accommodate different protein and lipid sources in the diet better than other marine fish species, without severely compromising the quality of the final edible product even under a lipid profile perspective.

Feeding trials on commercial size fish will be useful to assess the long-term effects of the diets herein tested and to establish whether the final edible product quality is affected by high inclusion of BSF meal in the diet of *M. cephalus*.

4 Conclusions

Overall, the findings obtained in the present study suggest that *M. cephalus* can tolerate the replacement of conventional ingredients of a low FM diet with partially defatted BSF meal.

The transcriptomic approach unveiled fine cell processes strictly related to dietary BSF meal, suggesting a transcriptional "tipping point" between 10% and 15% replacement, indicating hepatic metabolic reconfiguration at intermediate replacement levels and exacerbation at 20% replacement.

The consistent upregulation of protein quality control and oxidative phosphorylation across all levels indicates that the *M. cephalus*

Data availability statement

Raw sequencing transcriptome data is publicly available and deposited in the EBI ArrayExpress portal with accession ID E-MTAB-16923.

Ethics statement

The feeding trial experiment and all the procedures involving animals were carried out in strict accordance with EU legal

frameworks relating to the protection of animals used for scientific purposes (Directive 2010/63/EU). It was approved by the Italian Ministry of Health (n. 5598B.N.T61). The study was conducted in accordance with the local legislation and institutional requirements.

Author contributions

BR: Conceptualization, Methodology, Formal analysis, Validation, Writing – original draft. AM: Conceptualization, Methodology, Formal analysis, Validation, Writing – original draft. GM: Conceptualization, Supervision, Funding acquisition, Project administration, Writing – review & editing. LC: Methodology, Writing – review & editing. FG: Methodology, Validation, Writing – review & editing. RB: Methodology, Formal analysis, Funding acquisition, Writing – review & editing. AL: Methodology, Formal analysis, Writing – review & editing. DC: Writing – review & editing. FT: Writing – review & editing. SC: Supervision, Writing – review & editing.

Funding

The author(s) declared that financial support was received for this work and/or its publication. This work has been financially supported by the National Recovery and Resilience Plan (NRRP), Mission 4 Component 2 Investment 1.4 - Call for tender No. 3138 of 16 December 2021, rectified by Decree n.3175 of 18 December 2021 of the Italian Ministry of University and Research funded by the European Union – NextGenerationEU (Award Number: Project code CN_00000033,397 Concession Decree No. 1034 of 17 June 2022 adopted by the Italian Ministry of University and398Research, CUP D33C22000960007, Project title "National Biodiversity Future Center - NBFC").

Acknowledgments

The authors want to acknowledge Davide Salvati (Animal care) and Filippo Genovese for the technical support in managing fish facility during the feeding trial and Dr. Gioacchino Bono for freeze-drying of samples used for chemical analyses.

Conflict of interest

The authors declare that the research was conducted in the absence of any commercial or financial relationships that could be construed as a potential conflict of interest.

The author AL declared that they were an editorial board member of Frontiers, at the time of submission. This had no impact on the peer review process and the final decision.

Generative AI statement

The author(s) declared that generative AI was used in the creation of this manuscript. Generative AI (Microsoft Copilot) was used exclusively for language editing and improvement of readability, without affecting the scientific content, which remains the full responsibility of the authors.

Any alternative text (alt text) provided alongside figures in this article has been generated by Frontiers with the support of artificial intelligence and reasonable efforts have been made to ensure accuracy, including review by the authors wherever possible. If you identify any issues, please contact us.

Publisher's note

Supplementary material

The Supplementary Material for this article can be found online at: https://www.frontiersin.org/articles/10.3389/fmars.2026.1901130/full#supplementary-material

SUPPLEMENTARY FIGURE 1
Ridge plot of the 40 KEGG pathways statistically modulated in the BSF10 vs. BSF0 contrast. The y-axis lists enriched pathways ordered by descending normalized enrichment score (NES). The x-axis shows the log2 fold-change distribution of core enrichment genes associated with each pathway. Ridge height and spread reflect the gene distribution within each term, while fill color indicates the adjusted p-value (p.adjust).

SUPPLEMENTARY FIGURE 2
Gene Set Enrichment Analysis plots of KEGG pathways statistically modulated in the BSF15 vs. BSF0 contrast, sorted by ascending normalized enrichment score (NES), reported next to the pathway title. The top portion of each plot depict the profile of the running enrichment score; the middle panel presents the position of gene set members in the rank-ordered list; the bottom portion of each plot reports the value and distribution of the ranking metric.

SUPPLEMENTARY TABLE 1
Full results of the DESeq2 DGE analyses, per each contrast. "gene": NCBI gene ID; "baseMean": average of count values, normalized to size factors, across all samples; lfcSE: log2 fold change standard error; "stat": Wald test statistic; "pvalue": Wald test p-value; "padj": Benjamini-Hochberg adjusted p-value, FDR cut-off of 0.05; "name": gene name, when available.

SUPPLEMENTARY TABLE 2
Differentially expressed genes resulting from clustering the likelihood ratio test (LRT) results with degPatterns, with corresponding expression cluster assignment. Genes are ranked by statistical significance, with smaller p-values and adjusted p-values indicating stronger evidence of differential expression.

SUPPLEMENTARY TABLE 3
Results of the GSE analysis against the KEGG database conducted on all genes tested for differential gene expression ranked according to sign (log2 fold change) * (-log10(p-value)), per each contrast. Results are sorted by ascending NES. Significance assessed against a null distribution of enrichment scores generated by permuting ranked genes and recomputing the enrichment scores of the gene set for the permuted data. Benjamini-Hochberg FDR-adjusted p-value cut-off of 0.05.

References

Ackman, R. G. (2008). "Fatty acids in fish and shellfish," in *Fatty Acids in Foods and Their Health Implications*. Ed. C. K. Chow (CRC Press, Tylor & Francis Group, London, UK).

Akula, S. T., Nagaraja, A., Ravikanth, M., Kumar, N. G. R., Kalyan, Y., and Divya, D. (2021). Antifungal efficacy of lauric acid and caprylic acid - derivatives of virgin coconut oil against Candida albicans. *Biomed. Biotechnol. Res. J.* 5, 229–234. doi: 10.4103/bbrj.bbrj_65_21

Almeida, C., Rijo, P., and Rosado, C. (2020). Bioactive compounds from Hermetia Illucens larvae as natural ingredients for cosmetic applications. *Biomolecules* 10, 976. doi: 10.3390/biom10070976

AOAC (2019). *Official Methods of Analysis of AOAC International, Method 950.46: Moisture in Meat* (Rockville, MD: AOAC International).

Argyropoulou, V., Kalogeropoulos, N., and Alexis, M. N. (1992). Effect of dietary lipids on growth and tissue fatty acid composition of grey mullet (Mugil cephalus). *Comp. Biochem. Physiol. Part. A. Physiol.* 101, 129–135. doi: 10.1016/0300-9629(92)90640-C

Asche, F., and Tveterås, S. (2004). On the relationship between aquaculture and reduction fisheries. *J. Agric. Econ.* 55, 245–265. doi: 10.1111/j.1477-9552.2004.tb00095.x

Bakke, A. M., Glover, C., and Krogdahl, Å. (2010). "Feeding, digestion and absorption of nutrients," in *Fish Physiology* (Oxford: Elsevier Inc), 57–110. doi: 10.1016/S1546-5098(10)03002-5

Baruah, K., Norouzitallab, P., and Pal, A. K. (2017). "Development of low cost and eco-friendly feed for various candidate species for the sustainability of commercial aquaculture and reduction of aquatic pollution," in *Developing New Functional Food and Nutraceutical Products* (London: Elsevier), 441–453. doi: 10.1016/B978-0-12-802780-6.00024-9

Basak, S., and Duttaroy, A. K. (2020). Conjugated linoleic acid and its beneficial effects in obesity, cardiovascular disease, and cancer. *Nutrients* 12, 1913. doi: 10.3390/nu12071913

Basili, M., Randazzo, B., Caccamo, L., Guicciardi, O., Guizzardi, S., Meola, M., et al. (2025). Effect of graded inclusion of black soldier fly (Hermetia illucens, Linnaeus 1758) pre-pupae meal in diets for gilthead seabream (Sparus aurata, Linnaeus 1758) on gut microbiome and liver morphology. *Fish Physiol. Biochem.* 51, 85. doi: 10.1007/s10695-025-01485-z

Belghit, I., Liland, N., Gjesdal, P., Biancarosa, I., Menchetti, E., Li, Y., et al. (2019). Black soldier fly larvae meal can replace fish meal in diets of sea-water phase Atlantic salmon (Salmo salar). *Aquaculture* 503, 609–619. doi: 10.1016/j.aquaculture.2018.12.032

Belghit, I., Liland, N. S., Waagbø, R., Biancarosa, I., Pelusio, N., Li, Y., et al. (2018). Potential of insect-based diets for Atlantic salmon (Salmo salar). *Aquaculture* 491, 72–81. doi: 10.1016/j.aquaculture.2018.03.016

Bengtsson, H. (2025). R.utils: various programming utilities. doi: 10.32614/CRAN.package.R.utils

Bertini, A., Natale, S., Gisbert, E., Andrée, K. B., Concu, D., Dondi, F., et al. (2023). Exploring the application of Corynebacterium glutamicum single cell protein in the diet of flathead grey mullet (Mugil cephalus): effects on growth performance, digestive enzymes activity and gut microbiota. *Front. Mar. Sci.* 10, 1172505. doi: 10.3389/fmars.2023.1172505

Biswas, G., De, D., Thirunavukkarasu, A. R., Natarajan, M., Sundaray, J. K., Kailasam, M., et al. (2012). Effects of stocking density, feeding, fertilization and combined fertilization-feeding on the performances of striped grey mullet (Mugil cephalus L.) fingerlings in brackish water pond rearing systems. *Aquaculture* 338-341, 284–292. doi: 10.1016/j.aquaculture.2012.02.004

Bligh, E. G., and Dyer, W. J. (1959). A rapid method of total lipid extraction and purification. *Can. J. Biochem. Physiol.* 37, 911–917. doi: 10.1139/o59-099

Borland, M., Riesenbach, C., Shandilya, U., Chiasson, M. A., Karrow, N. A., and Huyben, D. (2024). Growth performance, hepatic gene expression, and plasma biochemistry of rainbow trout fed full-fat meal, defatted meal, oil and chitin from black soldier flies. *Comp. Immunol. Rep.* 6, 200149. doi: 10.1016/j.cirep.2024.200149

Borrelli, L., Varriale, L., Dipineto, L., Pace, A., Menna, L. F., and Fioretti, A. (2021). Insect derived lauric acid as promising alternative strategy to antibiotics in the antimicrobial resistance scenario. *Front. Microbiol.* 12, 620798. doi: 10.3389/fmicb.2021.620798

Bruni, L., Randazzo, B., Cardinaletti, G., Zarantoniello, M., Mina, F., Secci, G., et al. (2020). Dietary inclusion of full-fat Hermetia illucens prepupae meal in practical diets for rainbow trout (Oncorhynchus mykiss): lipid metabolism and fillet quality investigations. *Aquaculture* 529, 735678. doi: 10.1016/j.aquaculture.2020.735678

Caballero-Solares, A., Hall, J. R., Xue, X., Eslamloo, K., Taylor, R. G., Parrish, C. C., et al. (2017). The dietary replacement of marine ingredients by terrestrial animal and plant alternatives modulates the antiviral immune response of Atlantic salmon (Salmo salar). *Fish Shellfish Immunol.* 64, 24–38. doi: 10.1016/j.fsi.2017.02.040

Calduch-Giner, A., Bermejo-Nogales, A., Benedito-Palos, L., Estensoro, I., Ballester-Lozano, G., Sitja-Bobadilla, A., et al. (2013). Deep sequencing for de novo construction of a marine fish (Sparus aurata) transcriptome database with a large coverage of protein-coding transcripts. *BMC Genomics* 14, 178. doi: 10.1186/1471-2164-14-178

Caligiani, A., Marseglia, A., Leni, G., Baldassarre, S., Maistrello, L., Dossena, A., et al. (2018). Composition of black soldier fly prepupae and systematic approaches for extraction and fractionation of proteins, lipids and chitin. *Food Res. Int.* 105, 812–820. doi: 10.1016/j.foodres.2017.12.0122

Cao, X., Fang, W., Li, X., Wang, X., Mai, K., and Ai, Q. (2022). Increased LDL receptor by SREBP2 or SREBP2-induced lncRNA LDLR-AS promotes triglyceride accumulation in fish. *iScience* 25, 104670. doi: 10.1016/j.isci.2022.104670

Carpentier, J., Martin, C., Luttenschlager, H., Deville, N., Ferrara, D., Purcaro, G., et al. (2024). Common soluble carbohydrates affect the growth, survival, and fatty acid profile of black soldier fly larvae Hermetia illucens (Stratiomyidae). *Sci. Rep.* 14, 28157. doi: 10.1038/s41598-024-75730-5

Carter, C. G., Houlihan, D. F., Kiessling, A., Medale, F., and Jobling, M. (2001). Physiological effects of feeding. *Blackwell Sci. Ltd.*, 297–331. doi: 10.1002/9780470999516.ch13

Carvalho, M., Izquierdo, M., Valdés, M., Montero, D., and Farías, A. (2022). Oils combination with microalgal products as a strategy for increasing the N-3 long-chain polyunsaturated fatty acid content in fish oil-free diets for meagre (Argyrosomus regius). *Aquaculture Nutr.* 5275570, 18. doi: 10.1155/2022/5275570

Castro, L. F. C., Tocher, D. R., and Monroig, O. (2016). Long-chain polyunsaturated fatty acid biosynthesis in chordates: Insights into the evolution of Fads and Elovl gene repertoire. *Prog. Lipid Res.* 62, 25–40. doi: 10.1016/j.plipres.2016.01.001

Chen, H., and Boutros, P. C. (2011). VennDiagram: a package for the generation of highly-customizable Venn and Euler diagrams in R. *BMC Bioinf.* 12, 35. doi: 10.1186/1471-2105-12-35

Cho, J. H., and Kim, I. H. (2011). Fish meal – nutritive value. *J. Anim. Physiol. Anim. Nutr.* 95, 685–692. doi: 10.1111/j.1439-0396.2010.01109.x

Choi, B. D., Kang, S. J., Ha, Y. L., and Ackman, R. G. (1999). "Accumulation of conjugated linoleic acid (CLA) in tissues of fish fed diets containing various levels of CLA," in *Quality Attributes of Muscle Foods*. Eds. Y. L. Xiong, H. Chi-Tang and F. Shahidi (Springer, Boston, MA). doi: 10.1007/978-1-4615-4731-0_5

Chun, Y., and Kim, J. (2018). Autophagy: an essential degradation program for cellular homeostasis and life. *Cells* 7, 278. doi: 10.3390/cells7120278

Costa, R. S., Basto, A., Monteiro, M., Pinho, B., Sá, T., Santos, M. V., et al. (2026). Combining Hermetia illucens and Tenebrio molitor meals in diets for European seabass: effects on growth, nutrient utilisation, intestinal morphology and muscle quality. *Aquaculture* 610, 742899. doi: 10.1016/j.aquaculture.2025.742899

Crosetti, D. (2015). "Current state of grey mullet fisheries and culture," in *Biology, Ecology and Culture of Grey Mullets (Mugilidae)*, vol. 53. (CRC Press, Taylor & Francis, CRC Press (Taylor & Francis).

Desroches, S., Chouinard, P. Y., Galibois, I., Corneau, L., Delisle, J., Lamarche, B., et al. (2005). Lack of effect of dietary conjugated linoleic acids naturally incorporated into butter on the lipid profile and body composition of overweight and obese men. *Am. J. Clin. Nutr.* 82, 309–319. doi: 10.1093/ajcn.82.2.309

Dhiman, T. R., Anand, G. R., Satter, L. D., and Pariza, M. W. (1999). Conjugated linoleic acid content of milk from cows fed different diets. *J. Dairy Sci.* 82, 2146–2155. doi: 10.3168/jds.S0022-0302(99)75458-5

Diez, A., Menoyo, D., Pérez-Benavente, S., Calduch-Giner, J. A., Vega-Rubin de Celis, S., Obach, A., et al. (2007). Conjugated linoleic acid affects lipid composition, metabolism, and gene expression in gilthead sea bream (Sparus aurata L). *J. Nutr.* 137, 1363–1369. doi: 10.1093/jn/137.6.1363

Drosdowech, S., Bezner, S., Daisley, B., Chiasson, M., Easton, A., Rooney, N., et al. (2024). Influence of feed-ing black soldier fly (Hermetia illucens), cricket (Gryllodes sigillatus), and superworm (Zophobas morio) on the gut microbiota of rainbow trout (Oncorhynchus mykiss). *J. App. Microbiol.* 135, lxae295. doi: 10.1093/jambio/lxae295

Du, F., Xu, G., Nie, Z., Xu, P., and Gu, R. (2014). Transcriptome analysis gene expression in the liver of Coilia nasus during the stress response. *BMC Genomics* 15, 558. doi: 10.1186/1471-2164-15-558

Eslamloo, K., Xue, X., Hall, J. R., Smith, N. C., Caballero-Solares, A., Parrish, C. C., et al. (2017). Transcriptome profiling of antiviral immune and dietary fatty acid dependent responses of Atlantic salmon macrophage-like cells. *BMC Genomics* 18, 706. doi: 10.1186/s12864-017-4099-2

Esmail, S., and Manolson, M. F. (2021). Advances in understanding N-glycosylation structure, function, and regulation in health and disease. *Eur. J. Cell Biol.* 100, 151186. doi: 10.1016/j.ejcb.2021.151186

Essa, M. A. (1996). The effect of fish density and feeding frequency on both (Oreochromis niloticus and Mugil cephalus) fish reared as mixed culture in floating cages. *Bull. - Batt. Oceanogr. Fish Egypt.* 22, 181–197. doi: 10.1016/j.anres.2017.04.005

Ewald, N., Vidakovic, A., Langeland, M., Kiessling, A., Sampels, S., and Lalander, C. (2020). Fatty acid composition of black soldier fly larvae (Hermetia illucens) - possibilities and limitations for modification through diet. *Waste Manage.* 102, 40–47. doi: 10.1016/j.wasman.2019.10.014

FAO (2024). *The State of World Fisheries and Aquaculture 2024 - Blue Transformation in Action* (Rome: FAO). doi: 10.4060/cd0683en

Fox, S. E., Christie, M. R., Marine, M., Priest, H. D., Mockler, T. C., and Blouin, M. S. (2014). Sequencing and characterization of the anadromous steelhead (Oncorhynchus mykiss) transcriptome. *Mar. Genomics* 15, 13–15. doi: 10.1016/j.margen.2013.12.001

Gasco, L., Finke, M., and van Huis, A. (2018). Can diets containing insects promote animal health? *J. Insects Food Feed* 4, 1–4. doi: 10.3920/JIFF2018.x001

Gaullier, J. M., Berven, G., Blankson, H., and Gudmundsen, O. (2002). Clinical trial results support a preference for using CLA preparations enriched with two isomers rather than four isomers in human studies. *Lipids* 37, 1019–1025. doi: 10.1007/s11745-002-0995-y

Gaullier, J. M., Halse, J., Høye, K., Kristiansen, K., Fagertun, H., Vik, H., et al. (2005). Supplementation with conjugated linoleic acid for 24 months is well tolerated by and reduces body fat mass in healthy, overweight humans. *J. Nutr.* 135, 778–784. doi: 10.1093/jn/135.4.778

Goncalves, D. C., Lira, F. S., Carnevali, L. C. Jr., Rosa, J. C., Pimentel, G. D., and Seelaender, M. (2010). Conjugated linoleic acid: good or bad nutrient. *Diabetol. Metab. Syndr.* 2, 62. doi: 10.1186/1758-5996-2-62

Guillen, J., Asche, F., Borriello, A., Carvalho, N., Druon, J.-N., Garlock, T., et al. (2025). What is happening to the European Union aquaculture production? Investigating its stagnation and sustainability. *Aquaculture* 596, 741793. doi: 10.1016/j.aquaculture.2024.741793

Hasan, I., Rimoldi, S., Saroglia, G., and Terova, G. (2023). Sustainable fish feeds with insects and probiotics positively affect freshwater and marine fish gut microbiota. *Animals* 13, 1633. doi: 10.3390/ani13101633

Herdiyati, Y., Astrid, Y., Shadrina, A. A. N., Wiani, I., Satari, M. H., and Kurnia, D. (2021). Potential fatty acid as antibacterial agent against oral bacteria of Streptococcus mutans and Streptococcus sanguinis from basil (Ocimum americanum): *In vitro* and In silico studies. *Curr. Drug Discov. Technol.* 18, 532–541. doi: 10.2174/1570163817666200712171652

Heymann, F., and Tacke, F. (2016). Immunology in the liver - from homeostasis to disease. *Nat. Rev. Gastroenterol. Hepatol.* 13, 88–110. doi: 10.1038/nrgastro.2015.200

Houlihan, D. F., McMillan, D. N., and Laurent, P. (1986). Growth-rates, protein-synthesis, and protein — degradation rates in rainbow-trout-effects of body size. *Physiol. Zool.* 59, 482–493. doi: 10.1086/physzool.59.4.30158601

IJdema, F., Lievens, S., Smets, R., Poma, G., Van Der Borght, M., and Lievens, B. (2025). Modulating the fatty acid composition of black soldier fly larvae via substrate fermentation. *Animal* 19, 101383. doi: 10.1016/j.animal.2024.101383

ISTISAN (1996). *Metodi Di Analisi Utilizzati Per Il Controllo Chimico Degli Alimenti* (Rome: Istituto Superiore di Sanità). Rapporti ISTISAN 96/34.

Jin, A. H., Qian, Y. F., Ren, J., Wang, J. G., Qiao, F., and Zhang, M. L. (2023). PDK inhibition promotes glucose utilization, reduces hepatic lipid deposition, and improves oxidative stress in largemouth bass (Micropterus salmoides) by increasing pyruvate oxidative phosphorylation. *Fish Shellfish Immunol.* 140, 108969. doi: 10.1016/j.fsi.2023.108969

Karapanagiotidis, I. T., Bell, M. V., Little, D. C., and Yakupitiyage, A. (2007). Replacement of dietary fish oils by alpha-linolenic acid-rich oils lowers omega 3 content in tilapia flesh. *Lipids* 42, 547–559. doi: 10.1007/s11745-007-3057-1

Kelly, P. B., Reiser, R., and Hood, D. W. (1958). The origin and metabolism of marine fatty acids: The effect of diet on the depot fats of Mugil cephalus (The common mullet). *J. Am. Oil Chem. Soc* 35, 189–192. doi: 10.1007/BF02639824

Korotkevich, G., Sukhov, V., Budin, N., Shpak, B., Artyomov, M. N., and Sergushichev, A. (2021). "Fast gene set enrichment analysis," in *Biorxiv*. doi: 10.1101/060012

Lappano, R., Sebastiani, A., Cirillo, F., Rigiracciolo, D. C., Galli, G. R., Curcio, R., et al. (2017). The lauric acid-activated signaling prompts apoptosis in cancer cells. *Cell. Death Discov.* 3, 17063. doi: 10.1038/cddiscovery.2017.63

Le, A., and Dang, C. V. (2014). "Studying Myc's role in metabolism regulation," in *The Myc Gene*, vol. 1012. Eds. L. Soucek and N. Sodir (Totowa, NJ: Humana Press). doi: 10.1007/978-1-62703-429-6_14

Leone, A., Lecci, R. M., Durante, M., Meli, F., and Piraino, S. (2015). The bright side of gelatinous blooms: nutraceutical value and antioxidant properties of three Mediterranean jellyfish (Scyphozoa). *Mar. Drugs* 13, 4654–4681. doi: 10.3390/md13084654

Liu, J., Brinkman, D. B., Murray, A. M., Newbrey, M. G., Zhou, Z., Van Loon, L. L., et al. (2025). Marine origins and freshwater radiations of the otophysan fishes. *Sci. (New York N.Y.)* 390, 65–69. doi: 10.1126/science.adr4494

Love, M. I., Huber, W., and Anders, S. (2014). Moderated estimation of fold change and dispersion for RNA-seq data with DESeq2. *Genome Biol.* 15, 550. doi: 10.1186/s13059-014-0550-8

Luo, W., and Brouwer, C. (2013). Pathview: an R/Bioconductor package for pathway-based data integration and visualization. *Bioinformatics* 29, 1830–1831. doi: 10.1093/bioinformatics/btt285

Macusi, E. D., Cayacay, M. A., Borazon, E. Q., Sales, A. C., Habib, A., Fadli, N., et al. (2023). Protein fishmeal replacement in aquaculture: a systematic review and implications on growth and adoption viability. *Sustainability* 15, 12500. doi: 10.3390/su151612500

Magnanou, E., Klopp, C., Noirot, C., Besseau, L., and Falcón, J. (2014). Generation and characterization of the sea bass Dicentrarchus labrax brain and liver transcriptomes. *Gene* 544, 56–66. doi: 10.1016/j.gene.2014.04.032

Makkar, H. P. S., Tran, G., Heuzé, V., and Ankers, P. (2014). State-of-the-art on use of insects as animal feed. *Anim. Feed Sci. Technol.* 197, 1–33. doi: 10.1016/j.anifeedsci.2014.07.008

Mancini, S., Medina, I., Iaconisi, V., Gai, F., Basto, A., and Parisi, G. (2018). Impact of black soldier fly larvae meal on the chemical and nutritional characteristics of rainbow trout fillets. *Animal* 12, 1672–1681. doi: 10.1017/S1751731117003421

Marrero, M., Monroig, Ó., Pérez, J. A., Betancor, M. B., Galindo, A., Bolaños, A., et al. (2024). Dietary LC-PUFA and environmental salinity modulate the fatty acid biosynthesis capacity of the euryhaline teleost thicklip grey mullet (Chelon labrosus). *Comp. Biochem. Physiol. B. Biochem. Mol. Biol.* 269, 110865. doi: 10.1016/j.cbpb.2023.110865

Mendez Sanchez, C., de Lamo Castelvi, S., Alagappan, S., Hoffman, L. C., Yarger, O., and Cozzolino, D. (2025). Influence of the waste substrate and extraction method on the lipid profile of black soldier fly (Hermetia illucens). *J. Insects Food Feed* 12, 1343–1353. doi: 10.1163/23524588-bja10347

Mondall, A., Chakravortty, D., Mandal1, S., Bhattacharyya, S. B., and Mitra, A. (2015). Feeding ecology and prey preference of grey mullet, Mugil cephalus (Linnaeus 1758) in extensive brackish water farming system. *J. Mar. Sci. Res. Dev.* 6, 1. doi: 10.4172/2155-9910.1000178

Monroig, Ó., and Kabeya, N. (2018). Desaturases and elongases involved in polyunsaturated fatty acid biosynthesis in aquatic invertebrates: a comprehensive review. *Fish. Sci.* 84, 911–928. doi: 10.1007/s12562-018-1254-x

Moutinho, S., Oliva-Teles, A., Pulido-Rodríguez, L., Parisi, G., Magalhães, R., Monroig, Ó., et al. (2024). Effects of black soldier fly (Hermetia illucens) larvae oil on fillet quality and nutritional traits of gilthead seabream. *Aquaculture* 579, 740219. doi: 10.1016/j.aquaculture.2023.740219

Mu, Y. N., Ding, F., Cui, P., Ao, J. Q., Hu, S. N., and Chen, X. H. (2010). Transcriptome and expression profiling analysis revealed changes of multiple signaling pathways involved in immunity in the large yellow croaker during Aeromonas hydrophila infection. *BMC Genomics* 11, 506. doi: 10.1186/1471-2164-11-506

Mu, Y. N., Li, M. Y., Ding, F., Ding, Y., Ao, Y. Q., Hu, S. N., et al. (2014). De novo characterization of the spleen transcriptome of the large yellow croaker (Pseudosciaena crocea) and analysis of the immune relevant genes and pathways involved in the antiviral response. *PloS One* 5, e9747. doi: 10.1371/journal.pone.0097471

Nairuti, R. N., Musyoka, S. N., Yegon, M. J., and Opiyo, M. A. (2021). Utilization of black soldier fly (Hermetia illucens, Linnaeus) larvae as a protein source for fish feed - a review. *Aquac. Stud.* 22, AQUAST697. doi: 10.4194/AQUAST697

National Cancer Institute (NCI) Bioinformatics Training and Education Program (2023). *Pathways and Gene Sets: What is Functional Enrichment Analysis?* (Center for Cancer Research). Available online at: https://bioinformatics.ccr.cancer.gov/btep/pathways-and-gene-sets-what-is-functional-enrichment-analysis/ (Accessed June 20, 2026).

Near, T. J., Eytan, R. I., Dornburg, A., Kuhn, K. L., Moore, J. A., Davis, M. P., et al. (2012). Resolution of ray-finned fish phylogeny and timing of diversification. *PNAS* 109, 13698–13703. doi: 10.1073/pnas.1206625109

Neuwirth, E. (2022). RColorBrewer: ColorBrewer palettes. doi: 10.32614/CRAN.package.RColorBrewer

Nogales-Mérida, S., Gobbi, P., Józefiak, D., Mazurkiewicz, J., Dudek, K., Rawski, M., et al. (2019). Insect meals in fish nutrition. *Rev. Aquacult.* 11, 1080–1103. doi: 10.1111/raq.12281

Olsen, R. L., and Hasan, M. R. (2012). A limited supply of fishmeal: Impact on future increases in global aquaculture production. *TIFS* 27, 120–128. doi: 10.1016/j.tifs.2012.06.003

Olsen, R. E., Henderson, R. J., and McAndrew, B. J. (1990). The conversion of linoleic acid and linolenic acid to longer chain polyunsaturated fatty acids by Tilapia (Oreochromis) nilotica *in vivo*. *Fish Physiol. Biochem.* 8, 261–270. doi: 10.1007/BF00004465

Oren, O. H. (1981). "Aquaculture of grey mullets," in *Biol. Prog.* Ed. O. H. Oren (Cambridge: Cambridge Univ. Press), 411–493.

Oteri, M., Di Rosa, A. R., Lo Presti, V., Toscano, G., Giarratana, F., and Chiofalo, B. (2026). Partial fishmeal replacement with defatted Hermetia illucens meal in offshore-farmed gilthead seabream (Sparus aurata): effects on fillet quality and microbiological stability. *Fishes* 11, 211. doi: 10.3390/fishes11040211

Özogul, Y., and Özogul, F. (2007). Fatty acid profiles of commercially important fish species from the Mediterranean, Aegean and Black Seas. *Food Chem.* 100, 1634–1648. doi: 10.1016/j.foodchem.2005.11.047

Pantano, L. (2026). DEGreport: report of DEG analysis. doi: 10.18129/B9.bioc.DEGreport

Pulido-Rodriguez, L. F., Cardinaletti, G., Secci, G., Randazzo, B., Bruni, L., Cerri, R., et al. (2021). Appetite regulation, growth performances and fish quality are modulated by alternative dietary protein ingredients in gilthead sea bream (Sparus aurata) culture. *Animals* 11, 1919. doi: 10.3390/ani11071919

Quirós-Pozo, R., Roo, J., Izquierdo, M., Koven, W., Ramírez-Bolaños, S., Ventura-Castellano, A., et al. (2025). Effective complete replacement of fish oil by linseed oil in

diets for thick-lipped grey mullet (Chelon labrosus) juveniles reared at three environmental salinities. *Aquaculture* 594, 741425. doi: 10.1016/j.aquaculture.2024.741425

Ramos-Bueno, R. P., González-Fernández, M. J., Sánchez-Muros-Lozano, M. J., Garcia-Barroso, F., and Guil-Guerrero, J. L. (2016). Fatty acid profiles and cholesterol content of seven insect species assessed by several extraction systems. *Eur. Food Res. Technol.* 242, 1471–1477. doi: 10.1007/s00217-016-2647-7

Ramos-Júdez, S., Estévez, A., González-López, W.Á., and Duncan, N. (2023). Lipid and fatty acid composition of muscle, liver, ovary, and peritoneal fat in wild flathead grey mullet (Mugil cephalus) according to ovarian development. *Theriogenology* 198, 317–326. doi: 10.1016/j.theriogenology.2022.12.046

Randazzo, B., Caccamo, L., Carboni, S., Concu, D., Gai, F., Loi, B., et al. (2026). Defatted black soldier fly meal as a dietary protein source for grey mullet (Mugil cephalus): effects on growth performance, gut morphology, spleen and liver health. *Animals* 16, 1012. doi: 10.3390/ani16071012

Randazzo, B., Di Marco, P., Zarantoniello, M., Daniso, E., Cerri, R., Finoia, M. G., et al. (2023). Effects of supplementing a plant protein-rich diet with insect, crayfish or microalgae meals on gilthead sea bream (Sparus aurata) and European seabass (Dicentrarchus labrax) growth, physiological status and gut health. *Aquaculture* 575, 739811. doi: 10.1016/j.aquaculture.2023.739811

Rehati, A., Abuduaini, B., Liang, Z., Chen, D., and He, F. (2023). Identification of heat shock protein family A member 5 (HSPA5) targets involved in nonalcoholic fatty liver disease. *Genes Immun.* 24, 124–129. doi: 10.1038/s41435-023-00205-y

Reimand, J., Isserlin, R., Voisin, V., Kucera, M., Tannus-Lopes, C., and Rostamianfar, A. (2019). Pathway enrichment analysis and visualization of omics data using g:Profiler, GSEA, Cytoscape and EnrichmentMap. *Nat. Protoc.* 14, 482–517. doi: 10.1038/s41596-018-0103-9

Renna, M., Schiavone, A., Gai, F., Dabbou, S., Lussiana, C., Malfatto,, et al. (2017). Evaluation of the suitability of a partially defatted black soldier fly (Hermetia illucens L.) larvae meal as ingredient for rainbow trout (Oncorhynchus mykiss Walbaum) diets. *J. Anim. Sci. Biotechnol.* 8, 57. doi: 10.1186/s40104-017-0191-3

Rimoldi, S., Di Rosa, A. R., Oteri, M., Chiofalo, B., Hasan, I., Saroglia, M., et al. (2024). The impact of diets containing Hermetia illucens meal on the growth, intestinal health, and microbiota of gilthead seabream (Sparus aurata). *Fish Physiol. Biochem.* 50, 1003–1024. doi: 10.1007/s10695-024-01314-9

Romeo, S., and Valenti, L. (2025). Fifteen years of PNPLA3: Transforming hepatology through human genetics. *Liver Int.* 45, e70240. doi: 10.1111/liv.70240

Rosas, V. T., Monserrat, J. M., Bessonart, M., Magnone, L., Romano, L. A., and Tesser, M. B. (2019). Fish oil and meal replacement in mullet (Mugil liza) diet with Spirulina (Arthrospira platensis) and linseed oil. *Comp. Biochem. Physiol. Part. C. Toxicol. Pharmacol.* 218, 46–54. doi: 10.1016/j.cbpc.2018.12.009

Şengör, G. F., Özden, Ö., Erkan, N., Tüter, M., and Aksoy, H. A. (2003). Fatty acid compositions of flathead grey mullet (Mugil cephalus L. 1758) fillet, raw and beeswaxed caviar oils. *T. Turk. J. Fish. Aquat. Sci.* 3, 93–96.

Salem, M., Rexroad, C. E., Wang, J., Thorgaard, G. H., and Yao, J. (2010). Characterization of the rainbow trout transcriptome using Sanger and 454-pyrosequencing approaches. *BMC Genomics* 11, 564–574. doi: 10.1186/1471-2164-11-564

Sankappa, N. M., Lange, M. D., Yildirim-Aksoy, M., Eljack, R., Kucuktas, H., Beck, B. H., et al. (2024). Transcriptome analysis and immune gene expression of channel catfish (Ictalurus punctatus) fed diets with inclusion of frass from black soldier fly larvae. *Front. Physiol.* 14, 1330368. doi: 10.3389/fphys.2023.1330368

Sargent, J. R., Tocher, D. R., and Bell, J. G. (2002). "The lipids," in *Fish Nutrition*, *3rd edn*. Eds. J. E. Halver and R. W. Hardy (Academic, San Diego), 181–257.

Seierstad, S. L., Haugland, Ø., Larsen, S., Waagbø, R., and Evensen, Ø. (2009). Pro-inflammatory cytokine expression and respiratory burst activity following replacement of fish oil with rapeseed oil in the feed for Atlantic salmon (Salmo salar L.). *Aquaculture* 289, 212–218. doi: 10.1016/j.aquaculture.2008.12.004

Sissener, N. H., Ørnsrud, R., Sanden, M., Frøyland, L., Remø, S., and Lundebye, A.-K. (2018). Erucic acid (22:1n-9) in fish feed, farmed, and wild fish and seafood products. *Nutrients* 10, 1443. doi: 10.3390/nu10101443

Slowikowski, K. (2024).ggrepel: automatically position non-overlapping text labels with 'ggplot2'. Available online at: https://CRAN.R-project.org/package=ggrepel.

Smetana, S., Schmitt, E., and Mathys, A. (2019). Sustainable use of Hermetia illucens insect biomass for feed and food: Attributional and consequential life cycle assessment. *Resour. Conserv. Recycl.* 144, 285–296. doi: 10.1016/j.resconrec.2019.01.042

Soneson, C., Love, M. I., and Robinson, M. D. (2015). Differential analyses for RNA-seq: transcript-level estimates improve gene-level inferences. *F1000Research* 4, 1521. doi: 10.12688/f1000research.7563.2

Stubhaug, I., Tocher, D. R., Bell, J. G., Dick, J. R., and Torstensen, B. E. (2005). Fatty acid metabolism in Atlantic salmon (Salmo salar L.) hepatocytes and influence of dietary vegetable oil. *Biochim. Biophys. Acta* 1734, 277–288. doi: 10.1016/j.bbalip.2005.04.003

Sun, H., Dong, W., He, G., Long, Y., He, Y., Chen, Y., et al. (2024). Excessive level of dietary insect protein negatively changed growth metabolomic and transcriptomic profiles of largemouth bass (Micropterus salmoides). *Anim. Nutr.* 17, 397–407. doi: 10.1016/j.aninu.2024.03.014

Suryati, T., Julaeha, E., Farabi, K., Ambarsari, H., and Hidayat, A. T. (2023). Lauric acid from the black soldier fly (Hermetia illucens) and its potential applications. *Sustainability* 15, 10383. doi: 10.3390/su151310383

Tenenbaum, D., and Maintainer, B. (2025). *KEGGREST: Client-Side REST Access to the Kyoto Encyclopedia of Genes and Genomes (KEGG)*. R package version 1.52.2. doi: 10.18129/B9.bioc.KEGGREST

Tocher, D. R. (2003). Metabolism and functions of lipids and fatty acids in teleost fish. *Rev. Fish. Sci.* 11, 107–184. doi: 10.1080/713610925

Tocher, D., Agaba, M., Hastings, N., Bell, J. G., Dick, J. R., and Teale, A. J. (2001). Nutritional regulation of hepatocyte fatty acid desaturation and polyunsaturated fatty acid composition in zebrafish (Danio rerio) and tilapia (Oreochromis niloticus). *Fish Physiol. Biochem.* 24, 309–320. doi: 10.1023/A:1015022406790

Toral, P. G., Renna, M., Frutos, P., Gasco, L., and Hervás, G. (2025). Insect fat as feed: Potential to modify the fatty acid composition of animal-derived foods. *Anim. Nutr.* 22, 179–190. doi: 10.1016/j.aninu.2025.03.016

Truzzi, C., Girolametti, F., Annibaldi, A., Zarantoniello, M., Olivotto, I., Riolo, P., et al. (2023). Insect-based aquafeeds modulate the fatty acid profile of zebrafish: A comparison on the different life stages. *Anim. Feed Sci. Technol.* 305, 115761. doi: 10.1016/j.anifeedsci.2023.115761

Turchini, G. M., Torstensen, B. E., and Ng, W.-K. (2009). Fish oil replacement in finfish nutrition. *Rev. Aquac.* 1, 10–57. doi: 10.1111/j.1753-5131.2008.01001.x

Twibell, R. G., Watkins, B. A., Rogers, L., and Brown, P. B. (2000). Effects of dietary conjugated linoleic acids on hepatic and muscle lipids in hybrid striped bass. *Lipids* 35, 155–161. doi: 10.1007/BF02664765

Vallainc, D., Estevez, A., Ramos, S. J., Concu, D., Carboni, S., Duncan, N., et al. (2026). "Hatchery, nursery and grow-out techniques for the flathead grey mullet (Mugil cephalus)," in *FAO Fisheries and Aquaculture Technical Paper, No. 699* (FAO, Rome). doi: 10.4060/cd9536en

Varga, Á. T., Fabrikov, D., Sánchez-Muros, M. J., Jiménez, A. P., Palomares, E. R., Trenzado, C. E., et al. (2026). Substitution of fishmeal in Sparus aurata feed with Hermetia illucens meal elaborated by different successive post-harvest processing methods; nutrient utilization and growth indices, effects on intermediary metabolism and digestive chitinolytic activity. *Aquaculture* 619, 743802. doi: 10.1016/j.aquaculture.2026.743802

Whitfield, A. K., Panfili, J., and Durand, J.-D. (2012). A global review of the cosmopolitan flathead mullet Mugil cephalus Linnaeus 1758 (Teleostei: mugilidae), with emphasis on the biology, genetics, ecology and fisheries aspects of this apparent species complex. *Rev. Fish. Biol.* 22, 641–681. doi: 10.1007/s11160-012-9263-9

Wickham, H. (2025). *Stringr: Simple, Consistent Wrappers for Common String Operations*. Available online at: https://CRAN.R-project.org/package=stringr.

Wickham, H., Averick, M., Bryan, J., Chang, W., McGowan, L. D., François, R., et al. (2019). Welcome to the tidyverse. *J. Open Source Software* 4, 1686. doi: 10.21105/joss.01686

Wilke, C. (2025). *Ggridges: Ridgeline Plots in 'Ggplot2'*. Available online at: https://CRAN.R-project.org/package=ggridges.

Wu, N., Song, Y. L., Wang, B., Zhang, X. Y., Zhang, X. J., Wang, Y., et al. (2016). Fish gut-liver immunity during homeostasis or inflammation revealed by integrative transcriptome and proteome studies. *Sci. Rep.* 6, 36048. doi: 10.1038/srep36048

Xie, S., Liu, Y., Tian, L., Niu, J., and Tan, B. (2020). Low dietary fish meal induced endoplasmic reticulum stress and impaired phospholipids metabolism in juvenile pacific white shrimp, Litopenaeus vannamei. *Front. Physiol.* 11, 1024. doi: 10.3389/fphys.2020.01024

Xu, S., Hu, E., Cai, Y., Xie, Z., Luo, X., Zhan, L., et al. (2024). Using clusterProfiler to characterize multiomics data. *Nat. Protoc.* 19, 3292–3320. doi: 10.1038/s41596-024-01020-z

Xu, S., Wang, Q., Wen, S., Li, J., He, N., Li, M., et al. (2025). aplot: Simplifying the creation of complex graphs to visualize associations across diverse data types. *Innovation* 6, 100958. doi: 10.1016/j.xinn.2025.100958

Yu, G. (2025). *Enrichplot: Visualization of Functional Enrichment Result*. Available online at: https://yulab-smu.top/contribution-knowledge-mining/ (Accessed June 20, 2026).

Zarantoniello, M., Randazzo, B., Cardinaletti, G., Truzzi, C., Chemello, G., Riolo, P., et al. (2021). Possible dietary effects of insect-based diets across zebrafish (Danio rerio) generations: a multidisciplinary study on the larval phase. *Animals* 11, 751. doi: 10.3390/ani11030751

Zhang, S., Hulver, M. W., McMillan, R. P., Cline, M. A., and Gilbert, E. R. (2014). The pivotal role of pyruvate dehydrogenase kinases in metabolic flexibility. *Nutr. Metab. (Lond)* 11, 10. doi: 10.1186/1743-7075-11-10

Zheng, X., Torstensen, B. E., Tocher, D. R., Dick, J. R., Henderson, R. J., and Bell, J. G. (2005). "Environmental and dietary influences on highly unsaturated fatty acid biosynthesis and expression of fatty acyl desaturase and elongase genes in liver of Atlantic salmon (Salmo salar)," in *Biochim. Biophys. Acta*, vol. 1734. (Elsevier), 13–24. doi: 10.1016/j.bbalip.2005.01.006

Ziemann, M., Schroeter, B., and Bora, A. (2024). Two subtle problems with overrepresentation analysis. *Bioinf. Adv.* 4, vbae159. doi: 10.1093/bioadv/vbae159